



Invited Review

The role of infrequently mobile boulders in modulating landscape evolution and geomorphic hazards

Charles M. Shobe^{a,b,*}, Jens M. Turowski^a, Ron Nativ^{a,c,d}, Rachel C. Glade^e,
Georgina L. Bennett^f, Benedetta Dini^g

^a Helmholtz Centre Potsdam, GFZ German Research Centre for Geosciences, Potsdam, Germany

^b Department of Geology and Geography, West Virginia University, Morgantown, WV, USA

^c Institute of Earth and Environmental Science, University of Potsdam, Potsdam, Germany

^d Department of Earth and Environmental Sciences, Ben-Gurion University of the Negev, Beer Sheva, Israel

^e Department of Earth and Environmental Sciences, University of Rochester, Rochester, NY, USA

^f Geography, College of Life and Environmental Sciences, University of Exeter, Exeter, UK

^g School of Environmental Sciences, University of East Anglia, Norwich, UK



ARTICLE INFO

Keywords:

Geomorphology
Landscape evolution
Boulders
Rivers
Hillslopes
Channel-hillslope coupling
Geohazards

ABSTRACT

A landscape's sediment grain size distribution is the product of, and an important influence on, earth surface processes and landscape evolution. Grains can be large enough that the motion of a single grain, infrequently mobile in size-selective transport systems, constitutes or triggers significant geomorphic change. We define these grains as boulders. Boulders affect landscape evolution; their dynamics and effects on landscape form have been the focus of substantial recent community effort. We review progress on five key questions related to how boulders influence the evolution of unglaciated, eroding landscapes: 1) What factors control boulder production on eroding hillslopes and the subsequent downslope evolution of the boulder size distribution? 2) How do boulders influence hillslope processes and long-term hillslope evolution? 3) How do boulders influence fluvial processes and river channel shape? 4) How do boulder-mantled channels and hillslopes interact to set the long-term form and evolution of boulder-influenced landscapes? 5) How do boulders contribute to geomorphic hazards, and how might improved understanding of boulder dynamics be used for geohazard mitigation?

Boulders are produced on eroding hillslopes by landsliding, rockfall, and/or exhumation through the critical zone. On hillslopes dominated by local sediment transport, boulders affect hillslope soil production and transport processes such that the downslope boulder size distribution sets the form of steady-state hillslopes. Hillslopes dominated by nonlocal sediment transport are less likely to exhibit boulder controls on hillslope morphology as boulders are rapidly transported to the hillslope toe. Downslope transport delivers boulders to eroding rivers where the boulders act as large roughness elements that change flow hydraulics and the efficiency of erosion and sediment transport. Over longer timescales, river channels adjust their geometry to accommodate the boulders supplied from adjacent hillslopes such that rivers can erode at the baselevel fall rate given their boulder size distribution. The delivery of boulders from hillslopes to channels, paired with the channel response to boulder delivery, drives channel-hillslope feedbacks that affect the transient evolution and steady-state form of boulder-influenced landscapes. At the event scale, boulder dynamics in eroding landscapes represent a component of geomorphic hazards that can be mitigated with an improved understanding of the rates and processes associated with boulder production and mobility. Opportunities for future work primarily entail field-focused data collection across gradients in landscape boundary conditions (tectonics, climate, and lithology) with the goal of understanding boulder dynamics as one component of landscape self-organization.

* Corresponding author at: Department of Geology and Geography, West Virginia University, Morgantown, WV, USA
E-mail address: charles.shobe@mail.wvu.edu (C.M. Shobe).

1. Introduction

Illuminating Earth's history—and predicting its future—requires a thorough understanding of the processes that shape landscapes and deliver sediment from source to sink. Along with tectonics, climate, and biologic controls, Earth material (rock and sediment) properties exert a strong influence on the form and evolution of landscapes (e.g., Schanz and Montgomery, 2016; Roda-Boluda et al., 2018; Scott and Wohl, 2019; Ott, 2020; Zondervan et al., 2020). The size of sediment grains produced by the erosion of rock is one such property. Sediment grain size affects the efficiency and relative dominance of different geomorphic processes, and ultimately influences how landscapes respond to changes in their boundary conditions (e.g., Leopold, 1992; Sklar et al., 2017; DiBiase et al., 2018b).

Grain sizes in nature range from the sub-micron scale to blocks of rock tens of meters on a side (Fig. 1). When the largest grains in the grain size distribution (GSD) measure meters to tens of meters across, transport is often infrequent enough that the largest grains remain immobile over human observation timescales—and potentially much longer—in all but the most energetic environments (Fig. 2). These largest grains, which we call “boulders” without implying a specific size or shape, have long intrigued geomorphologists (e.g., Gilbert, 1877; Hack, 1965; Judd and Peterson, 1969; Rodine and Johnson, 1976; Beaty, 1989) who speculated about the production, transport, and degradation of large,

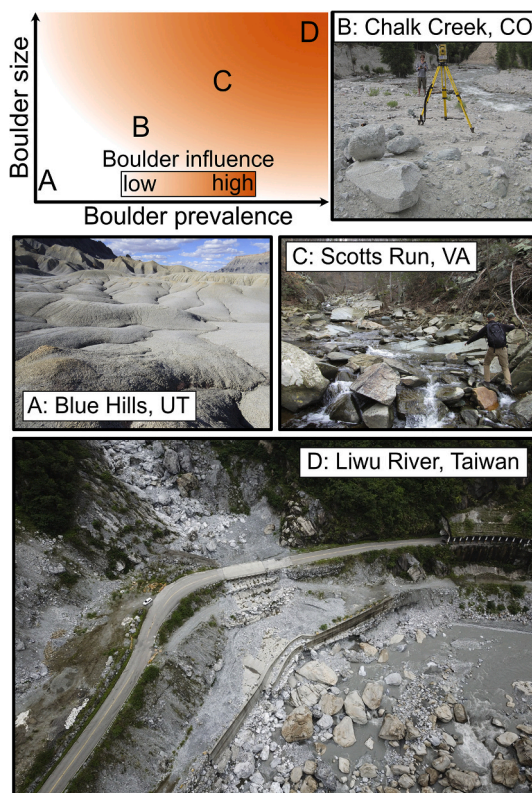


Fig. 1. Conceptual phase space showing the influence of boulders on landscape evolution as a function of boulder size and prevalence. Photographs correspond to labeled locations on the conceptual plot. A: The ephemeral fluvial landscape of the Blue Hills shale badlands shows an end-member in which small gravels are the largest sediment grains and boulder effects are expected to be negligible. B: A debris flow fan enters Chalk Creek, Colorado, delivering some large (1–2 m) boulders embedded in a much larger volume of fine-grained material. The boulders are long-lived in the valley whereas the fine-grained material is transportable by the creek's baseflow. C: Scotts Run erodes the pervasively fractured Mather Gorge formation, yielding large quantities of boulders up to several meters in size. D: Boulders tens of meters on a side entering the Liwu River, Taiwan from a debris flow channel.

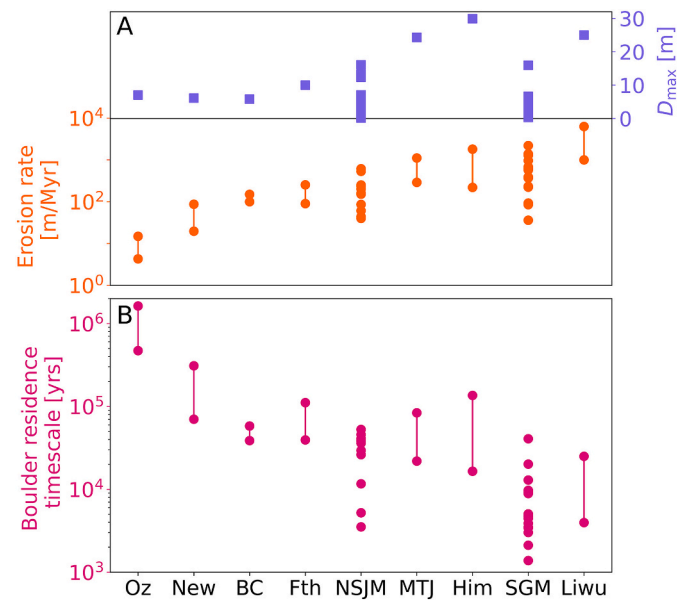


Fig. 2. A) Maximum observed grain sizes (D_{max}) and erosion rates from studies cited below. Oz: Ozarks, Arkansas, USA (Thaler and Covington, 2016; Beeson et al., 2017). New: New River, central Appalachians, Virginia, USA (Granger et al., 1997; Ward et al., 2005; Chilton and Spotila, 2020). BC: Boulder Creek, Colorado, USA (Schildgen et al., 2002; Dühnforth et al., 2012; Dethier et al., 2014; Shobe et al., 2016). Fth: Feather River, Sierra Nevada, USA (Hurst et al., 2012; Attal et al., 2015; Attal, 2017). Low erosion rates from “relict” uplands in the Feather basin are excluded because the largest boulders are observed in “adjusted” channel reaches (Attal et al., 2015; Attal, 2017). NSJM: Northern San Jacinto Mountains, California, USA (Neely et al., 2019; Neely and DiBiase, 2020). MTJ: Mendocino triple junction, northern California, USA (Balco et al., 2013; Roering et al., 2015; Shobe et al., 2020). Him: Nepal Himalaya (Godard et al., 2014; Huber et al., 2020). SGM: San Gabriel Mountains, California, USA (Neely et al., 2019; Neely and DiBiase, 2020). Liwu: Liwu River, Taiwan (Derrieux et al., 2014; Nativ et al., 2019). Erosion rates are the minimum and maximum for each area except for landscapes with paired erosion rate and grain size measurements available (NSJM and SGM; Neely and DiBiase, 2020). B) Boulder residence timescale calculated by dividing D_{max} by the erosion rate.

infrequently mobile grains and how they influence geomorphic processes and landscape evolution.

Understanding boulder dynamics and their effects on landscapes is challenging because boulders move infrequently, and because their motion typically occurs in destructive events like rockfalls and large floods (e.g., Cook et al., 2018; Huber et al., 2020). The advent of high-resolution topography and satellite imagery, structure-from-motion photogrammetry, new geochronologic techniques, and more powerful computer models has enabled a recent acceleration in research that seeks to understand boulder dynamics and their influence on the shape of landscapes through time. In this paper we review recent work with the goal of synthesizing observations and models and identifying fruitful avenues for future research.

1.1. What is a boulder?

The classic sedimentological definition of a boulder is a sediment grain with a diameter greater than 256 mm (Udden, 1914; Wentworth, 1922). The >256 mm size class has since been subdivided and repeatedly renamed (e.g., Blair and McPherson, 1999; Terry and Goff, 2014), but with 256 mm always remaining the lower bound of the boulder fraction. While this definition is useful from a sedimentological perspective, defining a strict size class does little good for the purposes of understanding from a process-based perspective how the largest sediment grains influence landscape evolution. In many steep, rapidly eroding landscapes, grains > 256 mm move in frequently recurring

floods as fluvial bedload (e.g., Lenzi, 2004; Turowski et al., 2009b) and undergo long-distance transport events on hillslopes (e.g., Bones, 1973; Statham, 1976; Bourrier et al., 2009; Copons et al., 2009). Because our goal is to understand how boulders affect landscape evolution, we need a more general definition rooted not in absolute grain size, but in the relationship between grain size and the pace and causes of landscape change.

While grain size is typically a smooth continuum, we can identify two conceptual end-members based on the idea that sediment transport is in many environments a size-selective process (e.g., Ashworth and Ferguson, 1989; Menting et al., 2015). In one end-member scenario, grains are small and mobile enough that geomorphic change is produced by the erosion and deposition of large numbers of grains. Alternatively, grains might be large enough that they alter the motion of smaller, more frequently mobile grains, and that the motion of a single grain constitutes or triggers significant geomorphic change. For the purposes of this review we define boulders as the latter. This definition does not require that boulders never move, especially over timescales long enough to incorporate rare transport events (Sklar et al., 2020); impressively large boulders can move during such events (e.g., Birkeland, 1968; Beaty, 1989; Turowski et al., 2009b; Cook et al., 2018; Huber et al., 2020; Greenbaum et al., 2020). Grains large enough to satisfy this definition are likely to remain immobile during the majority of transport events (Carling and Tinkler, 1998; Prancevic and Lamb, 2015), and their size and relative immobility combine to yield the geomorphic effects that we discuss.

The chosen conceptual definition satisfies the observation that the mobility of a given grain size class, as well as the contribution of a single grain's motion to geomorphic change, varies based on the erosion rate in a landscape (Fig. 2). In a drainage basin eroding at a few microns per year, the motion of a meter-scale grain is a rare event and constitutes substantial geomorphic change—change equivalent to or greater than that caused by the cumulative motion of smaller grains over many erosive events. That grain in that landscape is a boulder. In rapidly eroding orogens, the same grain might move many times per year; its motion would not constitute substantial geomorphic change and we would not consider it a boulder.

A compilation of boulder size and erosion rate data (Fig. 2) from eroding landscapes reveals that maximum boulder residence time—calculated by dividing maximum boulder size by background erosion rate—range from 10^3 to 10^6 years globally. While the largest boulders are typically found in actively uplifting orogens, the longest boulder residence times occur in more slowly eroding, post-orogenic landscapes (e.g., Mills, 1981; Granger et al., 2001; Thaler and Covington, 2016; Chilton and Spotila, 2020). The effects of boulders are expected to be most pronounced not simply in the landscape with the largest boulders, but in the landscape where boulders persist the longest. The relative (im) mobility of a given grain size fraction can further vary between landscapes due to tradeoffs between the frequency and intensity of transport events (e.g., Pfeiffer and Finnegan, 2018) and the effectiveness of boulder degradation processes like *in situ* weathering. A boulder that satisfies our conceptual definition can only be defined relative to other sediment grains experiencing the same forcing conditions in the same landscape.

The dependence of what constitutes a boulder on background erosion rates and sediment transport dynamics implies that rather than a universal size cutoff, boulders could be defined using the widespread convention of grain size percentiles (e.g., D_{50} is the median grain intermediate axis length from a given set of measurements (Wolman, 1954)). The most common statistic used to delineate the large end of the GSD is D_{84} , or the size of the 84th percentile of grains. This size class has been shown, for example, to be an effective proxy for boulder-related roughness in steep streams (Schneider et al., 2015). An alternative is to consider the D_{100} (e.g., Attal et al., 2015), the size of the largest grain measured, or any percentile in between. Larger percentiles will result in further reduced mobility—and potentially more clearly observable

boulder effects—in any size-selective sediment transport system, though percentiles approaching D_{100} become increasingly subject to sampling bias (Wilcock, 1992; Ferguson and Paola, 1997). We use D_{84} in parts of this review to match previous work, but emphasize that any strict cutoff is ultimately arbitrary, is vulnerable to arguments for incremental changes towards larger or smaller grains, and should be treated with caution. “Nature often comes to us as irreducible continua” (Gould, 1985).

A definition of a boulder rooted in the idea of size-selective transport implies that some amount of dispersion in the GSD (e.g., Spencer, 1963) is required to distinguish a consistently coarse GSD from one that includes both smaller, potentially more mobile grains and those that may be considered boulders by the criteria of decreased mobility and increased contribution to geomorphic change. Much of this review compares the behavior of geomorphic systems “with boulders” to those without. An increase in the size of any grain size percentile can be achieved by 1) coarsening the entire GSD or 2) coarsening only those grains that fall at or above the chosen percentile. While many of the boulder effects we describe apply to both cases, we focus on the second case, where the addition of boulders has increased the size of coarse grains relative to fine grains.

We move forward with the understanding that boulders:

1. are the largest and least mobile grains in a landscape,
2. affect the motion of smaller, more frequently mobile grains,
3. contribute to—or trigger—geomorphic change observable above the background rate of topographic change when they move,
4. may be represented by grain size percentiles at or above D_{84} in landscapes with substantial dispersion in the GSD, though any strict percentile cutoff represents the arbitrary discretization of a continuum, and
5. preferentially coarsen the upper end of the GSD, rather than the whole distribution, when delivered to a landscape.

1.2. Definition of scope

We focus on understanding how boulders are produced, influence geomorphic change, and affect the prevalence of geomorphic hazards. Boulders are generated by the fracturing of bedrock. While we review mechanisms of boulder production assuming the existence of suitably fractured rock, we refer readers to recent reviews treating fracture mechanics (Eppes and Keanini, 2017) and the influence of fractures on geomorphic processes (Scott and Wohl, 2019) for further details. Our review addresses how boulders alter landscape evolution once delivered to the landscape.

Boulders might have important geomorphic effects across process domains ranging from glacial (e.g., Anderson, 2014) and periglacial (e.g., Wilson et al., 2020) environments to coastlines (e.g., Cox et al., 2018). We restrict our review to non-glaciated, eroding landscapes. We focus on synthesizing work that treats boulder production, transport, and influence over landscape evolution on hillslopes and in river channels, as well as the hazards that stem from the presence of boulders.

The influence of boulders on landscape evolution processes and outcomes depends not only on boulder size, which governs their persistence in the landscape under a given weathering regime, but also on their prevalence at Earth's surface. We define prevalence as the volumetric proportion of all sediment grains that are long-lived boulders. Size and prevalence, functions of initial boulder size, resistance to degradation, and boulder delivery and export rates, conspire to influence landscape evolution. This idea can be conceptualized as a phase space that maps the importance of boulders to landscape evolution as a function of their size and prevalence (Fig. 1). We emphasize landscapes in which boulders are both large and prevalent because those are the landscapes in which boulder effects have been best explored.

This review uses the common conceptual framework of a landscape adjusting to some sustained increase in baselevel fall (or rock uplift

relative to baselevel) rate under a steady climatic forcing, in which a landscape will undergo transient response to that perturbation and ultimately achieve a time-averaged steady-state form (e.g., Whipple, 2001). This construct is useful because it allows conceptual comparison between the steady-state form of landscapes that can be considered fully adjusted to both their boulder prevalence and baselevel fall rate. We note, however, that the boulder dynamics and effects on geomorphic processes discussed here apply across all eroding landscapes regardless of their baselevel and climate history, including post-orogenic landscapes (Fig. 2) (e.g., Thaler and Covington, 2016; Chilton and Spotila, 2020) and postglacial landscapes with large supplies of glacial (e.g., Whitbread et al., 2015) or periglacial (e.g., Del Vecchio et al., 2018) boulders.

1.3. Structure and guiding questions

The paper follows a boulder's journey from production on a hillslope to its ultimate transport or degradation in a river channel, always focusing on how that boulder influences geomorphic processes and resulting landscape evolution. This review focuses on recent progress on the following guiding questions, each of which corresponds to a section of the paper:

1. What factors control boulder production on eroding hillslopes and the subsequent downslope evolution of the boulder size distribution? (section 2)
2. How do boulders influence hillslope processes and long-term hillslope evolution? (section 3)
3. How do boulders influence fluvial processes and river channel shape? (section 4)
4. How do boulder-mantled channels and hillslopes interact to set the long-term form and evolution of boulder-influenced landscapes? (section 5)
5. How do boulders contribute to geomorphic hazards, and how might improved understanding of boulder dynamics be used for geohazard mitigation? (section 6)

2. Boulder production and size evolution on hillslopes

What factors control boulder production on eroding hillslopes and the subsequent downslope evolution of the boulder size distribution?

Hillslopes make up the vast majority of the land surface. While boulders can be produced in river channels through plucking of the bedrock by erosive flows (see review by Lamb et al. (2015)), the areal dominance of hillslopes implies that they host most boulder production. Rates of boulder production, as well as the size distribution of boulders yielded, govern boulder effects on the long-term evolution of hillslopes and rivers (e.g., Granger et al., 2001; Bennett et al., 2016; Thaler and Covington, 2016; Glade et al., 2017; Shobe et al., 2020).

2.1. Boulder production

The size distribution of sediment—including boulders—produced on eroding hillslopes is a function of erosion rate, bedrock properties, climate, and biology (e.g., Marshall and Sklar, 2012; Riebe et al., 2015; Sklar et al., 2017). In a given rock type and climate, boulders are most likely to be produced on slopes experiencing erosion rates sufficient to outpace soil production and potential boulder weathering in the critical zone (Linton, 1955; Fletcher and Brantley, 2010; Brocard et al., 2016; Sklar et al., 2017), expose bedrock (Neely and DiBiase, 2020), and/or fail in bedrock landslides (Attal et al., 2015).

Many boulder-rich landscapes exhibit steep hillslopes that experience landslides, rockfalls, dry ravel, and other nonlocal transport processes (e.g., Korup et al., 2006; Korup, 2006; Ouimet et al., 2007; Bennett et al., 2016; DiBiase et al., 2017; Spreafico et al., 2017; Roda-Boluda et al., 2018; Finnegan et al., 2019; Shobe et al., 2020; Neely and

DiBiase, 2020). Bedrock landslides are particularly efficient agents of boulder production because they access rock from depth that is able to bypass the soil column and escape substantial weathering (e.g., Marc et al., 2021). Bedrock landslides are also likely to preferentially occur in pervasively fractured rock already amenable to boulder production (Clarke and Burbank, 2011).

Boulders on hillslopes are often associated with the cropping out of favorably fractured rock units presumed to be especially resistant to weathering. These units survive exhumation to the surface and release boulders in rockfall events when underlying strata are eroded away leaving a steep topographic gradient susceptible to rockfall or toppling (Spreafico et al., 2017; Ward, 2019). While comminution of rock occurs during landslide and rockfall events (Davies et al., 1999; Ruiz-Carulla et al., 2017), mapping of boulders in deposits at the base of steep hillslopes consistently shows that grains tens of meters on a side emerge intact from rockfalls (Ruiz-Carulla et al., 2017) and landslides (Finnegan et al., 2019; Shobe et al., 2020).

Key bedrock properties like rock type and the density of macro-scale discontinuities set the maximum grain size within a given landscape and modulate the effects of erosional controls (Molnar et al., 2007; DiBiase et al., 2018b; Roda-Boluda et al., 2018; Neely et al., 2019; Scott and Wohl, 2019; Neely and DiBiase, 2020; Verdian et al., 2020; Marc et al., 2021). Climatically determined weathering efficiency (Anderson, 1998; Hales and Roering, 2007; Eppes and Keanini, 2017; Lamp et al., 2017; Messenzehl et al., 2018) governs whether rock detached at the surface will reflect *in situ* fracture density, or whether it will take the form of smaller fragments or corestones within a weathered matrix (Fletcher and Brantley, 2010). Boulders result from a set of fracture density and weathering conditions under which pieces of rock can be detached from the bedrock rather than simply weathering *in situ*, while being large and weathering-resistant enough to remain immobile once detached.

2.2. Downslope evolution of boulder size

Once boulders are released on hillslopes, the boulder size distribution as a function of distance downslope is set by a combination of boulder weathering and transport.

2.2.1. Downslope size evolution due to weathering

Boulders on hillslopes degrade by chemical (e.g., Fritz and Mohr, 1984; Darmody et al., 2005) and mechanical weathering (e.g., Eppes et al., 2010; Eppes and Griffing, 2010; McGrath et al., 2013; Putkonen et al., 2014; Aldred et al., 2016; Lamp et al., 2017). Recent work suggests that mechanical weathering occurs through the steady growth of cracks at low stresses (Eppes and Keanini, 2017) such as those driven by solar insolation cycles (Aldred et al., 2016). The potential dependence of cracking rates on climate (e.g., Eppes et al., 2020), in addition to the known effects of lithology (e.g., Perras and Diederichs, 2014), indicates that the control exerted by boulder weathering processes over the downslope boulder size distribution is globally variable. Even in the absence of boulder transport, mechanical weathering can cause downslope fining in cases where boulder position on the hillslope is correlated with exposure time. This would be the case on a slope below a boulder-yielding outcrop that produces boulders of a single size and retreats horizontally over time (Ward et al., 2011; McGrath et al., 2013; Duszyński and Migoń, 2015; Glade and Anderson, 2018; Ward, 2019).

The size distribution of boulders on a hillslope likewise evolves due to downslope boulder transport by local transport processes—those for which particle travel distance distributions are thin-tailed such that particle motion depends only on local slope—like small-scale sliding or toppling events, as well as nonlocal processes—those for which particle travel distance distributions are heavy-tailed such that particle motion depends on the distribution of slopes along a travel pathway—like landsliding, rockfall, or dry ravel (e.g., Foufoula-Georgiou et al., 2010; Tucker and Bradley, 2010; Gabet and Mendoza, 2012; Furbish and Roering, 2013; Doane et al., 2018; Furbish et al., 2020a, 2020b). The

transition between local and nonlocal transport processes is thought to be primarily a function of hillslope gradient, where nonlocal transport dynamics tend to dominate as hillslopes steepen (Furbish et al., 2020a).

2.2.2. Downslope size evolution due to local transport

On hillslopes too gently sloped to experience nonlocal boulder transport, boulders move repeatedly by toppling or sliding over short distances (on the order of one grain diameter or smaller) (e.g., Glade et al., 2017). Boulders may undergo downslope creep as part of a larger mass of slowly moving soil (Dini et al., 2021). They may topple as soil preferentially erodes from their downslope side and builds up on their upslope side. Evidence for how the frequency and displacement of such local transport events varies with grain size is lacking, but preliminary modeling studies suggest that size-selective hillslope transport may occur, resulting in faster transport of smaller grains relative to the largest boulders (Glade et al., 2017; Glade and Anderson, 2018). Assuming that the size of boulders produced along a hillslope is spatially uniform, size-selective transport favoring smaller grains would result in a downslope-finishing GSD where the largest boulders are found near their bedrock source.

2.2.3. Downslope size evolution due to nonlocal transport

When hillslopes approach angles at which nonlocal sediment transport processes dominate, the largest boulders are typically found at the base of the slope (e.g., Neely and DiBiase, 2020). This represents the culmination of a downslope coarsening trend driven by the fact that larger particles have greater momentum, are less likely to be disentrained by surface roughness elements (e.g., Roth et al., 2020), and therefore experience greater travel distances than smaller particles (e.g., Kirkby and Statham, 1975; DiBiase et al., 2017; Messenzehl et al., 2018; Neely and DiBiase, 2020; Roth et al., 2020). Such momentum-driven downslope transport due to landsliding, rockfall, or dry ravel can result in boulder fragmentation due to impacts against other rocks along the hillslope or crushing within a larger failure mass (e.g., Davies et al., 1999; Locat et al., 2006; Ruiz-Carulla et al., 2017; Ruiz-Carulla and Corominas, 2020), but observed downslope coarsening trends indicate that fragmentation effects do not outcompete the greater travel distances of large grains (e.g., Ruiz-Carulla et al., 2015; Marc et al., 2021).

2.3. Case studies of controls on boulder production and downslope transport

2.3.1. Rock property controls on boulder size

Though few studies focus explicitly on the largest grains, a recent proliferation of grain size measurements on hillslopes has begun to advance our understanding of how rock properties influence boulder production. Roda-Boluda et al. (2018) showed that grain sizes—represented by the D_{84} —weathered from bedrock correlate with Schmidt hammer rebound values, an empirical point measurement of the uniaxial compressive strength of *in situ* bedrock. They further showed that landslides, the size and prevalence of which are influenced by lithology and rock strength, yield coarser sediment than hillslope weathering and that this coarsening is greater in units with greater rock strength. Roda-Boluda et al. (2018) argue for the long-suggested idea that rocks with higher measured rock strength deliver larger grain sizes. This result is consistent with other measurements from landslide deposits (e.g., Attal and Lavé, 2006; Locat et al., 2006; Shobe et al., 2020; Marc et al., 2021) that do not explicitly measure rock strength but find lithologic controls on the size of the largest grains yielded from hillslopes.

Other recent field measurements collected across a wide range of lithologies and climatic conditions have quantified the extent to which grain sizes—and the size of the largest grains—on talus slopes at the base of bedrock cliffs reflect bedrock fracture spacing. Verdian et al. (2020) found that talus grain sizes, including the largest grains, closely match outcrop fracture spacing, implying that little weathering occurs during

rock exposure in outcrop or during the detachment process. They also showed that both fracture spacing and grain size clustered tightly by lithology. This confirms the importance of rock type, and potentially lithology-dependent fracture spacing, in setting the initial size distribution of boulders released from bedrock.

2.3.2. Erosion rate, fracture spacing, and size-selective transport controls on boulder size

Emerging remote sensing techniques are enabling larger-scale field analyses that can reveal how boulder production and transport processes interact to set the boulder size distribution across landscapes. Neely and DiBiase (2020) recently analyzed the relative influence of erosion rate, fracture density, and size-selective transport on grain sizes yielded from eroding hillslopes. They combined cosmogenic radionuclide erosion rate measurements, fracture spacing measurements derived from structure-from-motion photogrammetry, and grain sizes measured from imagery and in the field. They found that grain sizes—including the coarse fraction as represented by the D_{84} —coarsen with distance down hillslopes/talus slopes and colluvial channels such that grain sizes at the colluvial-to-fluvial process transition nearly approach the hillslope outcrop fracture spacing. This suggests that nonlocal transport processes on hillslopes (e.g., dry ravel) and in colluvial channels (e.g., debris flows) preferentially transport boulders relative to smaller grain sizes, and result in GSDs broadly controlled by fracture spacing.

Neely and DiBiase (2020) were also able to isolate the influence of erosion rate on grain size by comparing channel-head grain size measurements across basins with a large range of erosion rates. They observed a positive relationship between erosion rate and grain size up to the erosion rate at which the channel-head grain size approached the measured fracture spacing. At erosion rates greater than this critical value, grain size remained constant regardless of further increases in erosion rate. Neely and DiBiase (2020) linked this transition to the appearance of steep, bare-bedrock hillslopes on which grains released from the bedrock spend minimal time weathering in the soil column before moving downslope. Their results quantify how boulder production is controlled by the interplay between erosion rate and rock properties, with fracture spacing setting the maximum boulder size and erosion rate governing the extent to which grains moving down hillslopes reflect that spacing.

2.3.3. Transport process controls on boulder size

Even in landscapes with steep, erosive hillslopes, a given process domain can experience locally variable transport dynamics that influence the boulder size distribution. We present new boulder size data on a rapidly eroding, earthflow-prone threshold hillslope (Bennett et al., 2016) in the Eel River basin (California, USA). We mapped all visible boulders—approximately 400—on the hillslopes in the study area (Fig. 3), with boulders located both on the surface of active and dormant earthflows as well as on the surrounding hillslopes. In addition, approximately 400 boulders were mapped in the channel. This landscape is unique because all mapped boulders are making the same journey from hillslope to channel, but some are traveling by earthflow and some are not.

Comparison of boulder size distributions observed on earthflows, on immobile portions of the hillslopes, and in the channel (Fig. 3) suggests that boulder sizes are similar between earthflows and the channel, whereas boulders on immobile hillslopes tend to be larger. It is possible that the presence of the largest grains on hillslopes results from a survey area bias (more hillslope area than earthflow or river area surveyed), but we view this as unlikely given the large number of boulders mapped and the greater proportion of grains > 5 m on the hillslope relative to the earthflow and channel. The similarity in sizes between earthflow and channel boulders can be explained by the fact that earthflows move downslope at average rates of over a meter per year in this landscape (Bennett et al., 2016), which likely results in earthflow-derived boulders being over-represented in in-channel boulder deposits.

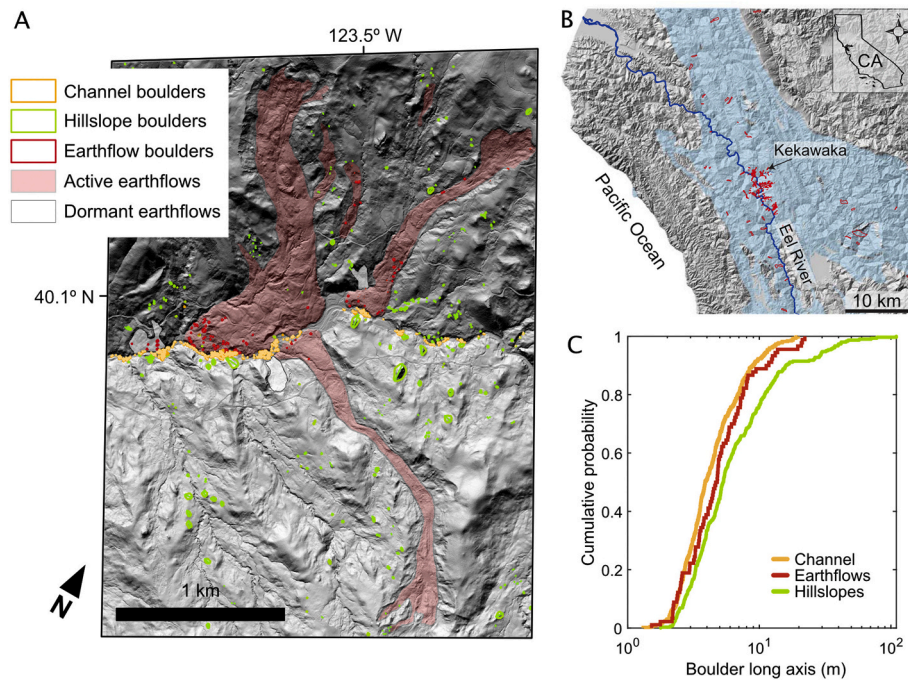


Fig. 3. A) Google Earth mapping of boulders on earthflows (red), hillslopes (green) and in the channel (yellow) from the Kekawaka tributary of the Eel River, California. B) Location of the study area with earthflows outlined in red and the earthflow-prone Franciscan Mélange rock unit shown in blue. C) Cumulative probability distributions of boulder sizes on earthflows, hillslopes, and in the channel.

The greater size of boulders on immobile hillslopes relative to boulders in earthflows is somewhat counterintuitive; one might expect the opposite because fast-moving earthflows may reduce the amount of time that boulders undergo weathering between their exposure at the surface and their deposition in a channel. If a flux steady state exists between boulder production and evacuation, the smaller earthflow boulders could suggest that weathering may be more effective within earthflows or that size segregation dynamics differ between processes, hiding the largest boulders beneath the surface in earthflows but not on hillslopes. Increased moisture might aid chemical weathering and flow deformation could accelerate physical boulder breakdown. It is also an interesting possibility that the causal relationship between geomorphic process and grain size is reversed: a correlation between substrate boulder size and bulk hillslope strength could cause earthflows to preferentially form in areas with smaller boulders in the subsurface and therefore weaker overall hillslopes (e.g., Scheingross et al., 2013).

Classifying boulder size data by geomorphic process domain raises important questions about how the boulder size distribution responds to, and potentially influences, transport process dominance even within a single landscape subject to collective, nonlocal transport processes. More work is needed to untangle variable boulder production and transport dynamics not just across, but also within, geomorphic environments.

2.4. Summary: Boulder production and size evolution on hillslopes

The boulder size distribution produced in a given landscape depends on erosion rate (Fletcher and Brantley, 2010; Neely and DiBiase, 2020), climate (Brocard et al., 2016; Sklar et al., 2017), rock type (Roda-Boluda et al., 2018; Shobe et al., 2020; Verdian et al., 2020), and fracture density (Neely and DiBiase, 2020; Verdian et al., 2020). These factors control the boulder size distribution in the near subsurface and set the mechanism of boulder production (rockfall, landslide, or corestone weathering). The downslope distribution of boulder sizes is then set by size-selective transport dynamics during boulder production and any subsequent downslope motion, as well as boulder degradation through

chemical and mechanical weathering. The boulder size distribution is more likely to fine downslope in slowly eroding, low-gradient landscapes where local transport processes dominate. Boulder sizes are more likely to coarsen downslope as hillslopes steepen and nonlocal, momentum-driven transport processes dominate. The initial boulder size distribution and its modification downslope play an important role in setting the form and evolution of boulder-influenced hillslopes (Ward et al., 2011; Glade et al., 2017; Glade and Anderson, 2018), channels (e.g., Johnson et al., 2009; Brocard and Van der Beek, 2006; Attal, 2017), and landscapes (e.g., DiBiase et al., 2018b; Shobe et al., 2020).

3. The effects of boulders on hillslope evolution

How do boulders influence hillslope processes and long-term hillslope evolution?

While most literature in hillslope geomorphology focuses on soil-mantled slopes with grain sizes so small that their motion can be treated using continuum mechanics approaches, the importance of large boulders to hillslope evolution has long been acknowledged. Early work posited that lateral erosion of bedrock cliffs depends on removal of the debris mantle beneath them via weathering and/or transport (King, 1953; Koons, 1955; Wahrhaftig, 1965; Moon, 1984; Selby, 1987; Howard and Kochel, 1988). More generally, the mobility and susceptibility to weathering of large boulders are thought to set the pace of hillslope evolution as well as steady-state hillslope form.

Through the use of cosmogenic radionuclides, detailed mapping, and numerical modeling, recent work has begun to quantitatively document the armoring effects of boulders (Granger et al., 2001; Marchetti et al., 2012; DiBiase et al., 2018a; Chilton and Spotila, 2020) and to explore their influence on long-term landscape evolution (Ward et al., 2011; Glade et al., 2017; Glade and Anderson, 2018; Glade et al., 2019). Here we review processes governing the evolution of boulder-strewn hillslopes, first focusing on hillslopes dominated by local sediment transport and then on steep, near-threshold hillslopes dominated by nonlocal sediment transport. We then synthesize findings from recent numerical and field studies detailing long-term hillslope evolution in the presence

of boulders.

3.1. Hillslope sediment dynamics

Production and transport of mobile material from bedrock drive hillslope evolution in eroding landscapes. When fine-grained material—hereafter referred to as soil—is fine enough that large numbers of grains can be collectively mobilized by common transport processes (Furbish et al., 2020a) and occupies gentle enough slopes that it undergoes local transport (e.g., Foufoula-Georgiou et al., 2010; Tucker and Bradley, 2010), soil transport can be treated using continuum approaches where downslope soil flux depends on local slope. In steep landscapes near the threshold for mass wasting, sediment transport becomes nonlocal and canonical hillslope evolution equations no longer apply (e.g., Tucker and Bradley, 2010; Doane et al., 2018; Furbish et al., 2020a). We discuss separately the influence of boulders on hillslopes dominated by local and nonlocal transport.

3.1.1. Hillslopes dominated by local sediment transport

Soil motions have traditionally been characterized as a diffusion-like process where soil flux increases with slope (Culling, 1960). Surface processes such as rainsplash, freeze/thaw cycles, wetting/drying cycles, and bioturbation are assumed to cause soil particles to creep, or move randomly in a net downslope direction. Soil creep is captured in a rule that relates soil flux q_{soil} (in units of M/(LT)) to topographic slope S_h . Written in one dimension, this rule states that:

$$q_{\text{soil}}(x) = kS_h(x), \quad (1)$$

where $S_h(x) = dz/dx$ with z being the topographic elevation as a function of x , the horizontal distance from the hillslope divide. Here k is a constant of proportionality—assumed here to be spatially uniform for simplicity—that represents the efficiency of soil transport, and $S_h(x)$ is taken to be positive in the downslope direction. This is directly inspired by heat diffusion (Jaeger and Carslaw, 1959)—the topographic slope is asserted to take the place of a temperature gradient (Culling, 1960; Dietrich et al., 2003). At steady state, defined where the soil thickness does not change through time, the soil flux must accommodate soil added through bedrock weathering. Thus $q_{\text{soil}} = kS_h(x) = wx$, where w is the vertical weathering rate of bedrock (Gilbert, 1909). The accumulation of soil flux with downslope distance results in a prediction of increasing slope with distance, $S_h(x) = \frac{w}{k}x$, which in one dimension describes a convex-upward parabolic hillslope.

The linear dependence of soil flux on slope (Eq. 1) can be replaced with a nonlinear dependence that accounts for the observation that soil fluxes increase nonlinearly as hillslopes approach a critical slope S_c and transition from local to nonlocal (e.g., landsliding) processes (Andrews and Bucknam, 1987; Roering et al., 1999, 2001a, 2001b):

$$q_{\text{soil}}(x) = \frac{kS_h(x)}{1 - (|S_h(x)|/S_c)^2}. \quad (2)$$

While Equation 2 is a local rule in the sense that soil flux depends only on local slope, it attempts to account for the effects of nonlocal, collective transport processes that keep hillslopes below a critical angle (the critical angle is not equivalent to the threshold angle for hillslope failure *sensu* Burbank et al. (1996); see Roering et al. (1999)). The linear and nonlinear flux approaches can produce hillslope forms ranging from parabolic (the linear model) to a parabolic hilltop with linear sideslopes (the nonlinear model) (Andrews and Bucknam, 1987; Martin and Church, 1997; Roering et al., 1999, 2001b,a; Dietrich et al., 2003). Recent studies focusing on grain-to-grain interactions have shown that gravity alone can cause soil to move downhill (Houssais and Jerolmack, 2017; BenDror and Goren, 2018; Ferdowsi et al., 2018; Deshpande et al., 2020), inspiring flux rules that move beyond Equations 1 and 2 to reproduce the shape of slopes shaped by both creep and hillslope failure (Ferdowsi et al., 2018).

3.1.2. Hillslopes dominated by nonlocal sediment transport

On slopes where sediment grains experience nonlocal transport—for example, steep slopes where dry ravel dominates (e.g., Gabet, 2003; Gabet and Mendoza, 2012; DiBiase et al., 2017)—recent work has begun to acknowledge the role of individual sediment particles, developing frameworks that explicitly treat discrete grain motions as a function of grain size, surface roughness, and the distribution of slopes a particle experiences during its journey downslope (e.g., Gabet and Mendoza, 2012; Furbish and Roering, 2013; Doane et al., 2018; Roth et al., 2020; Furbish et al., 2020a, 2020b). As hillslopes exceed some threshold slope dictated by their material strength, sediment and bedrock begin to undergo mass failure processes consisting of downslope motion that is both collective and nonlocal (e.g., Burbank et al., 1996; Andrews and Bucknam, 1987; Roering et al., 2001b; Neely and DiBiase, 2020). Mathematical formulations that incorporate the transition to nonlocal transport at steep slopes typically predict steady-state hillslopes with a convex ridgetop and planar sideslopes (e.g., Roering et al., 2007; Carretier et al., 2016).

3.2. Boulder effects on hillslope sediment dynamics

Recent studies have begun to address how large, relatively immobile boulders on hillslopes modify—or in some cases invalidate—classic assumptions in hillslope geomorphology (e.g., Ward et al., 2011; Glade et al., 2017; DiBiase et al., 2018a; Chilton and Spotila, 2020). Boulders affect hillslope sediment transport by altering 1) weathering of—and soil production from—underlying bedrock, and 2) transport of smaller, frequently mobile sediment grains (Figs. 4 and 5A). Proposed physical mechanisms for boulder control on hillslope evolution include: a decrease in erosion by overland flow due to increased surface roughness (Bunte and Poesen, 1993; Michaelides and Martin, 2012), protection of underlying soil from rainsplash (Poesen et al., 1994), interlocking of sediment grains due to overburden weight and a subsequent decrease in erosion rate (e.g., Bruthans et al., 2014), damming of soil behind boulders acting as obstacles (Glade et al., 2017; Chilton and Spotila, 2020), boulder-induced increases in land surface roughness that inhibit nonlocal downslope motion—for example by dry ravel (Gabet, 2003; DiBiase et al., 2017), and protection of underlying bedrock from weathering (Granger et al., 2001; Chilton and Spotila, 2020). Many of these effects are difficult to observe directly, leading most researchers to seek the signature of boulder effects in the hillslope topography itself.

3.3. Boulder effects on the evolution of hillslope topography

3.3.1. The evolution of hillslopes dominated by local sediment transport

Field studies show that the relief of soil-mantled hillslopes tends to increase with boulder prevalence, suggesting that boulders inhibit soil production and transport and force hillslopes to steepen to achieve erosion rates matching the baselevel fall rate (Granger et al., 2001; Crouvi et al., 2015; Glade et al., 2017; Glade and Anderson, 2018; DiBiase et al., 2018a). During transient landscape adjustment, boulders can even decrease erosion rates to the point that the landscape experiences a topographic inversion. This occurs when boulder-mantled valleys erode much more slowly than boulder-free high points, leading to a reversal of the high and low points in the landscape (e.g., Ward et al., 2011; Marchetti et al., 2012).

Numerical modeling studies have explored the time-evolution of boulder-mantled hillslopes dominated by local sediment transport. Most modeling studies treat the simplified case of hillslope evolution beneath a boulder-yielding cliff (Ward et al., 2011; Glade et al., 2017; Glade and Anderson, 2018; Glade et al., 2019). Boulder cover on hillslopes in such simplified cliff-source models—assuming that boulders do not undergo nonlocal transport upon release from the cliff—is typically greater near the boulder source at the hillcrest due to preferential deposition near the source (Ward et al., 2011) and/or the combined effects of boulder weathering and intermittent downslope transport (Glade et al., 2017). A

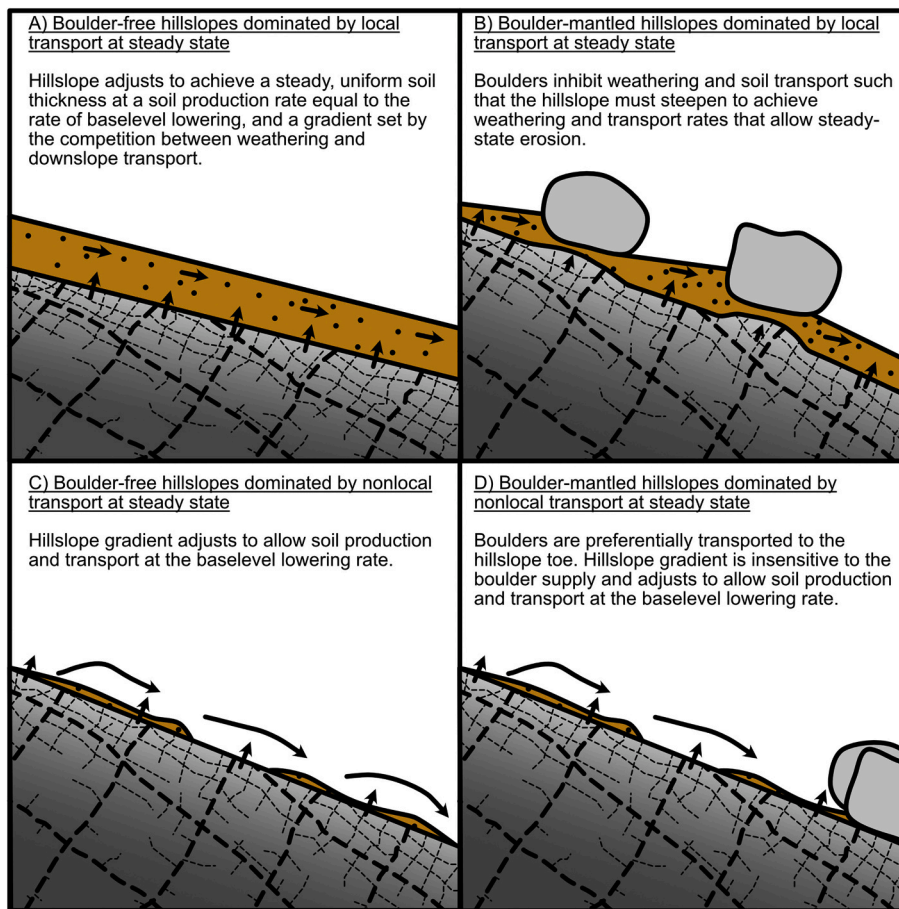


Fig. 4. The influence of boulders on hillslope processes for hillslopes dominated by local (A and B) and nonlocal (C and D) transport. A) a length of hillslope (small enough that convexity due to accumulating soil flux is neglected) equilibrated to its baselevel forcing with a steady and uniform soil production rate and soil depth. B) boulders inhibit weathering and soil transport, forcing the hillslope to steepen and adjust its soil thickness to achieve steady-state erosion conditions. In the boulder-mantled hillslope case, steady state must be thought of in a space- and time-averaged sense as boulders may occupy different locations at different times. C) a length of boulder-free hillslope dominated by nonlocal transport, showing the patchy soil cover often observed as hillslopes approach their threshold angle (e.g., Neely and DiBiase, 2020). D) The form of steep hillslopes dominated by nonlocal transport is insensitive to the boulder supply because boulders are preferentially transported to the hillslope toe.

downslope decrease in boulder cover and/or size results in hillslopes that experience stronger boulder effects, and therefore enhanced steepening to achieve a given erosion rate, at the top of the slope than at the bottom. Using the framework of Equation 1 for simplicity, boulders effectively decrease the soil transport efficiency k , causing the landscape to steepen most where boulders are largest or most prevalent. If boulders become smaller or less prevalent downslope, the steepening effect decreases, resulting in a decrease in slope with distance from the crest (Figs. 5B and 6A). Such a relationship between the downslope boulder size distribution and hillslope form has been observed in numerical models and comparisons with small amounts of field data (Glade et al., 2017; Glade and Anderson, 2018), but has not been extensively tested.

3.3.2. Steady-state hillslopes dominated by local sediment transport

In the case of steady and uniform climatic and tectonic boundary conditions, boulder-mantled hillslopes can reach a quasi-steady state (Ward et al., 2011; Glade et al., 2017; Glade and Anderson, 2018; Ward, 2019) in which time-averaged hillslope form and erosion rates do not change with time. Steady-state hillslope topography adjusts such that soil production and transport rates enable every point along the hillslope to lower at the baselevel fall rate under a given set of boulder size, prevalence, and resistance conditions (Ward et al., 2011; Glade et al., 2017; Glade and Anderson, 2018; DiBiase et al., 2018a). This condition is described as “quasi-steady state” (Glade and Anderson, 2018) because modeling efforts have focused on laterally retreating layered rock landforms (Fig. 5B), but true steady state would exist on hillslopes in other lithologic settings through the same boulder production and transport mechanisms.

In one dimension, the steepening of boulder-mantled hillslopes at a given erosion rate can be conceptualized using a simple geometric

expression that expands on Equation 1 to account for the effects of boulders on soil production and transport (Glade et al., 2017):

$$S_h(x) = \frac{w}{k}x + \frac{D(x)}{L(x)}. \quad (3)$$

The first term on the right hand side gives the solution for a boulder-free hillslope (Gilbert, 1909). The second term, in which D is boulder size at a given position x and L is downslope boulder spacing at that position, reflects the contribution of boulder effects (reduction in soil production rate, damming of soil) to hillslope steepening. When this second term nears zero, as in the case of small boulders or very widely spaced boulders, steady-state hillslope form is not expected to deviate significantly from the boulder-free case. Large and/or densely spaced boulders result in the boulder term overwhelming the soil term, leading to substantially steepened hillslopes. Changes in $D(x)$ and $L(x)$ along the hillslope govern how boulder-mantled hillslope form differs from the boulder-free case (Fig. 6).

If there exists a downslope decrease in boulder size or spacing—expected if boulders get progressively smaller downslope by weathering (McGrath et al., 2013) and/or size-dependent transport (Duszyński and Migoń, 2015)—steady-state hillslopes are concave up (Figs. 5B and 6A) due to the increased steepening near the hillcrest required to achieve a given erosion rate in the presence of many large boulders (Eq. 3). Such concave-up hillslopes are commonly observed in boulder-influenced landscapes (e.g., King, 1957; Selby, 1987; Howard and Selby, 1994; Ward et al., 2011; Glade et al., 2017) and differ from the convex-up form predicted for soil-mantled hillslopes. When the boulder term is large relative to the soil term and unchanging downslope, slope becomes nearly independent of distance such that the profile of a heavily boulder-mantled hillslope is predicted to be linear

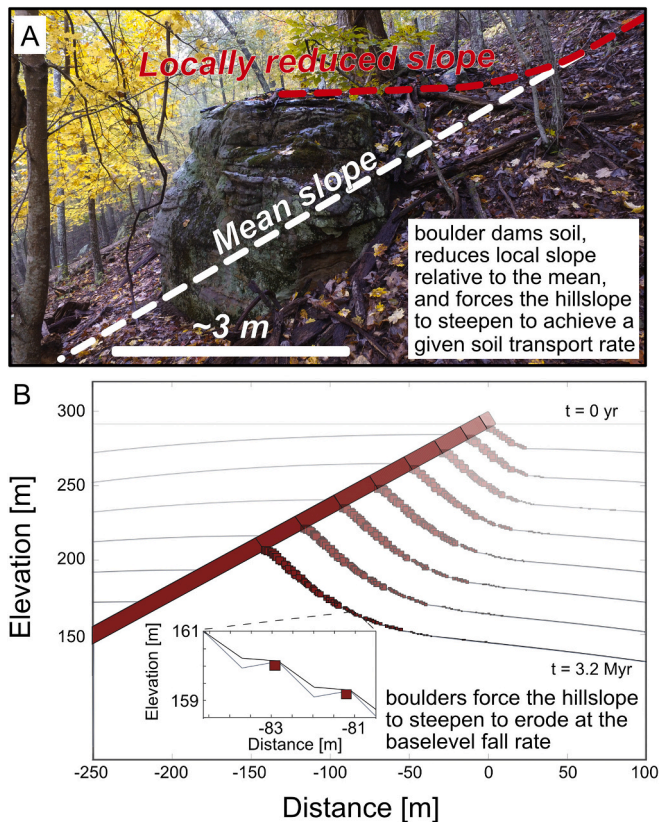


Fig. 5. A) A boulder damming soil on Gap Mountain, Virginia (modified from Fig. 4C in Chilton and Spotila (2020)). B) Numerical simulations of boulder-mantled hillslope evolution showing the development of a quasi-steady-state hillslope (modified from Fig. 3 in Glade et al. (2017)). In this simulation, boulders are released from a dipping, resistant rock layer. The landform achieves a steady-state form with respect to the retreating source of boulders. Boulders increase hillslope steepness and relief by reducing the bedrock weathering rate beneath boulders and by inhibiting soil transport (inset in B) as shown in A). The hillslope is concave-up due to the downslope-fining boulder size distribution that results in greater boulder-induced steepening closer to the hilltop.

(Fig. 6B). In locations where the largest boulders travel the farthest upon release from their source, for example where rockfall and landsliding dominate boulder delivery (e.g., Erismann and Abele, 2001; Copons et al., 2009; Duszyński et al., 2017), boulder size might increase downslope. Assuming that boulder spacing remains constant, this would lead to a convex-up steady-state hillslope (Fig. 6C) even in the presence of a strong boulder influence on erosion processes. Equation 3 captures the behavior of one-dimensional models for boulder-mantled hillslope evolution assuming that hillslopes remain below threshold gradients and are dominated by local transport processes (Glade et al., 2017). While the general prediction of boulder-mantled hillslopes being steeper than hillslopes without boulders is supported by field data (Granger et al., 2001; DiBiase et al., 2018a), Equation 3 has not been explicitly tested in the field.

Though examples of perfect steady state in nature are likely rare, understanding how boulder-mantled hillslopes approach a steady form is important because it complicates the simple idea that boulders decrease erosion rates. At steady state, the erosion rate is the rate of baselevel fall regardless of boulder dynamics; the relevant question is how hillslopes adjust their steady-state form in the presence of boulder effects. Field studies have indeed shown that large boulders occupy steeper parts of the landscape (Granger et al., 2001; Crouvi et al., 2015; Glade et al., 2017; DiBiase et al., 2018a), suggesting that rather than topography only dictating where boulders deposit, boulders can also

control the long-term shape and evolution of topography. Steep, boulder-strewn areas can erode at the same rate as, or slower than, portions of the landscape with gentler slopes (Granger et al., 2001; DiBiase et al., 2018a). This suggests that the topography and spatial distribution of boulder sizes co-evolve to account for boulder-related inhibition of soil production and transport in addition to climatic and tectonic boundary conditions, producing steady-state landforms that reflect boulder production and transport dynamics.

3.3.3. The evolution of hillslopes dominated by nonlocal sediment transport

On steep hillslopes dominated by nonlocal sediment transport, the largest boulders tend to be found the farthest downslope (e.g., Neely and DiBiase, 2020) due to the dominant effects of relative roughness (the ratio of grain size to surface roughness) on travel distance (e.g., Kirkby and Statham, 1975; DiBiase et al., 2017). While downslope coarsening of boulder sizes can occur on hillslopes dominated by local sediment transport as long as there is some nonlocal component of boulder delivery (e.g. a cliff that drops boulders onto the hillslope), the effects of boulders are thought to be different on hillslopes dominated by nonlocal transport across the GSD. These hillslopes exhibit a planar morphology set by the erosion rate at the hillslope toe, the frictional strength of the bedrock and/or overlying sediment, and the roughness of the hillslope surface which contributes to the disentrainment of sediment grains in motion (e.g., DiBiase et al., 2017; Doane et al., 2018; Roth et al., 2020; Furbish et al., 2020a, 2020b).

On hillslopes that experience nonlocal transport but are below the threshold angle for mass failure, the boulder size distribution may help govern the maximum hillslope angle by setting the surface roughness, and therefore the disentrainment rate of sediment (e.g., Doane et al., 2018), along the hillslope. The effect would however likely be less pronounced than on local-transport-dominated hillslopes because the largest boulders in nonlocal transport systems are efficiently transported to the hillslope toe. In cliff-talus systems, boulder size may influence the angle of mass failure, with larger boulders yielding slopes with greater strength and therefore greater failure angles (e.g., Carson, 1977; Church et al., 1979).

The presence of planar hillslopes in landscapes dominated by nonlocal transport and mass wasting suggests that boulders may not leave a distinctive geomorphic signature on transient or steady hillslope form in these regions. If hillslopes are consistently close to the threshold angle for failure and boulders are efficiently transported downslope, hillslope form will simply reflect the threshold angle (Fig. 4C and 4D). The dominance of nonlocal transport processes that efficiently evacuate boulders to the hillslope toe, coupled with the strong influence of mass-wasting on hillslope form, may prevent the boulder size distribution from feeding back on local hillslope topography to the extent hypothesized for hillslopes dominated by local transport. When the largest boulders are efficiently delivered to the hillslope toe, their most significant effect on hillslope form likely comes from their control over hillslope baselevel by affecting fluvial erosion.

3.4. Summary: The effects of boulders on hillslope evolution

Boulders inhibit soil production and transport, forcing hillslopes to adjust their form to erode at a given baselevel fall rate when local transport dynamics dominate (Figs. 4A, 4B, and 5). Boulder size and spacing set the degree to which a hillslope must adjust its steady-state form relative to a case without boulders, such that the downslope distributions of boulder size and spacing set hillslope relief, slope, and concavity (Fig. 6). The dynamics of production, weathering, and transport determine the boulder size distribution, which controls hillslope transience and steady-state form in potentially predictable ways. When nonlocal transport dominates, boulders may efficiently bypass the hillslope and hillslope form is set by its failure angle rather than the boulder size distribution (Fig. 4C and 4D). Boulder dynamics on hillslopes set the size distribution of boulders delivered to river channels (e.g., Attal et al.,

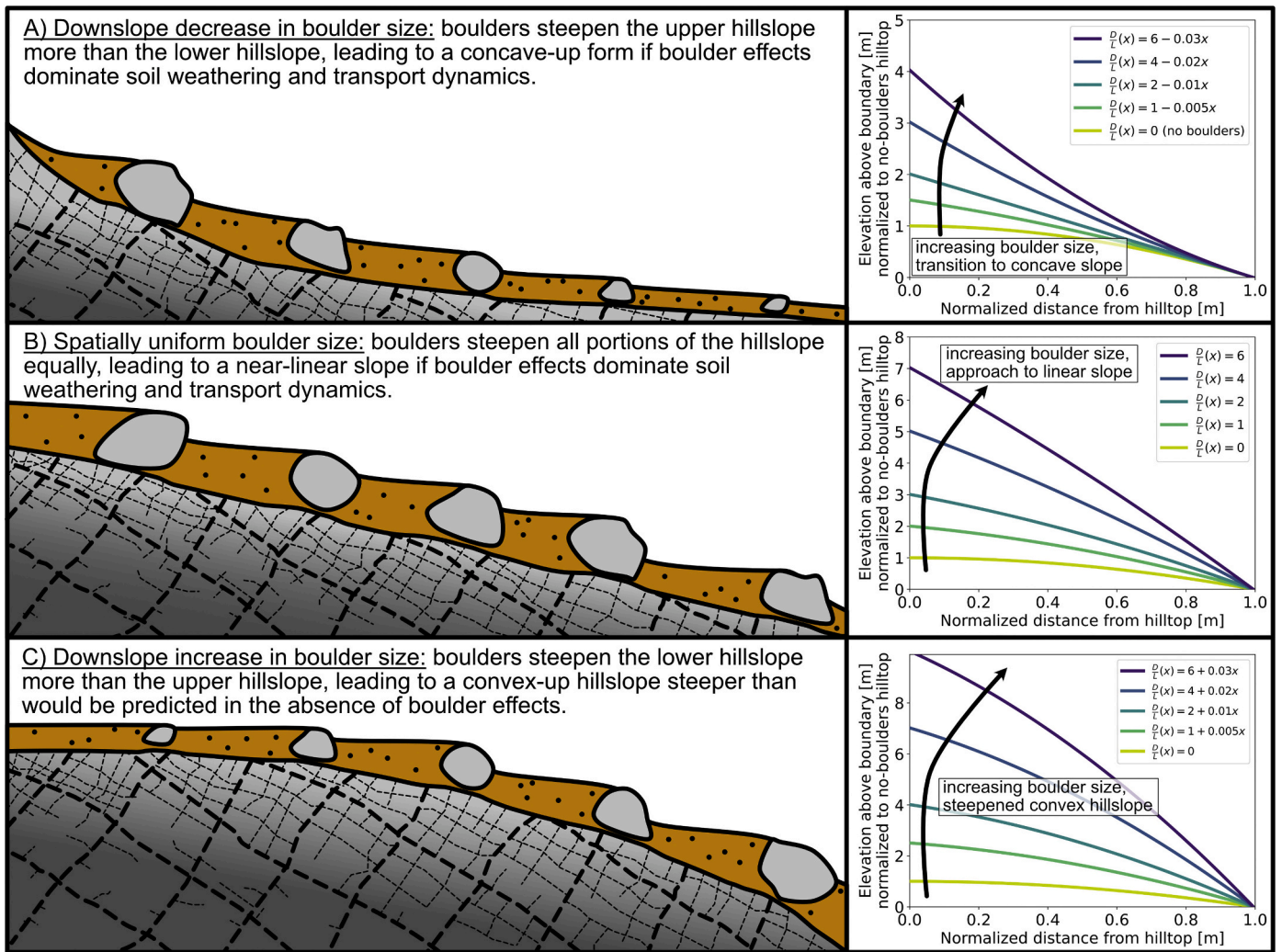


Fig. 6. The influence of the downslope boulder size/spacing distribution on the steady-state topography of hillslopes dominated by local sediment transport, as predicted by Equation 3 for a case when the right-hand term ($\frac{D(x)}{L(x)}$; boulder controls on slope) dominates over the left-hand term ($\frac{D(x)}{L(x)}$; weathering and soil transport controls on slope). Under such conditions, a downslope-fining boulder size distribution leads to a concave-up hillslope (A), a spatially uniform boulder size distribution leads to a linear hillslope (B), and a downslope-coarsening boulder size distribution leads to a convex-up hillslope (C). Right panels show the approach to each end-member hillslope form as a function of the downslope distribution of boulder sizes $D(x)$ and spacings $L(x)$, as represented by a linear function treating $\frac{D}{L}(x)$ as a function of downslope distance x . Steady-state hillslope profiles were computed analytically by integrating Equation 3 with a linear function for $\frac{D}{L}(x)$ as shown in the plot legends, and $\frac{D}{L} = 0.01$. The no-boulders case is the same profile in each plot. Hillslope form becomes progressively more dominated by boulder effects as $\frac{D}{L}(x)$ increases. The same is not true for hillslopes dominated by nonlocal transport, where the largest boulders are delivered to the hillslope toe and do not feed back on hillslope form.

2015; Sklar et al., 2017; Glade et al., 2019; Neely and DiBiase, 2020) such that the evolution of boulder-mantled hillslopes has important downslope implications. If boulder transport outpaces weathering, boulder size reduction may be minimal. If weathering outpaces transport, boulders may be easily mobilized by the time they reach channels. Hillslope morphology may encode signatures of these two end-member cases (Glade et al., 2017, 2019).

4. Reach-scale effects of boulders in rivers

How do boulders influence fluvial processes and river channel shape?

Boulders can be delivered to river channels after a journey down a hillslope (Section 2), directly delivered by landsliding, rockfall, or debris flows (Korup et al., 2006; Ouimet et al., 2007; Bennett et al., 2016; Finnegan et al., 2019; Shobe et al., 2020), or produced *in situ* by plucking (e.g., Lamb et al., 2015; Wilkinson et al., 2018). Boulders are thought to

be important elements in setting channel morphology in mountain streams (Montgomery and Buffington, 1997; Palucis and Lamb, 2017; Polvi, 2021), and to influence channel form and erosion dynamics in large rivers (e.g., Howard and Dolan, 1981; Cook et al., 2018; Turzewski et al., 2019; Shobe et al., 2020). In addition, boulder placement is frequently used as a method for stabilizing channel beds and banks (e.g., Lenzi, 2002; Pagliara and Chiavaccini, 2006; Chin et al., 2009) for restoration.

Here we focus on the influence of boulders that can be observed at the channel reach ($10^0 - 10^3$ m) scale, with effects that have broader relevance for landscape evolution. We describe how boulder-rich channels differ from boulder-free channels in terms of reach-scale average flow velocity, bedload transport, and channel morphology.

4.1. Effects on flow velocity

Flow velocity is a key hydraulic parameter. It scales both with the

energy available in the stream and the bed shear stress. The effect of the relative flow depth, defined as the ratio of flow depth to the size of the roughness elements such as boulders, on flow velocity scaling was recognized early (e.g., Bathurst, 1978; Hey, 1979; Judd and Peterson, 1969) but still presents open questions for research. The presence of boulders increases relative roughness, causing reductions in flow velocity at a given water discharge per unit width (Fig. 7). A comprehensive overview of previous data and models for flow resistance in boulder-bed channels has been given by Ferguson (2007), and Kalathil and Chandra (2019) recently reviewed hydrodynamics in step-pool channels specifically. We discuss flow velocity as a function of discharge in boulder-influenced channels using the dimensionless parameters suggested by Rickenmann and Recking (2011) based on earlier ideas of Ferguson (2007). The use of these parameters was subsequently justified from dimensional analysis by Nitsche et al. (2012). The dimensionless flow velocity V^* is

$$V^* = \frac{V}{\sqrt{gS_r D_{84}}} \quad (4)$$

Here, V is the flow velocity, g is the acceleration due to gravity, S_r is the channel bed slope and the roughness size D_{84} is the grain size that is larger than 84% of the grains found on the channel bed. We use D_{84} to conform to previous work while acknowledging that there are challenges to defining boulders using any single grain-size statistic (Section 1.1). The dimensionless unit discharge q^* is

$$q^* = \frac{q}{\sqrt{gS_r D_{84}^3}} \quad (5)$$

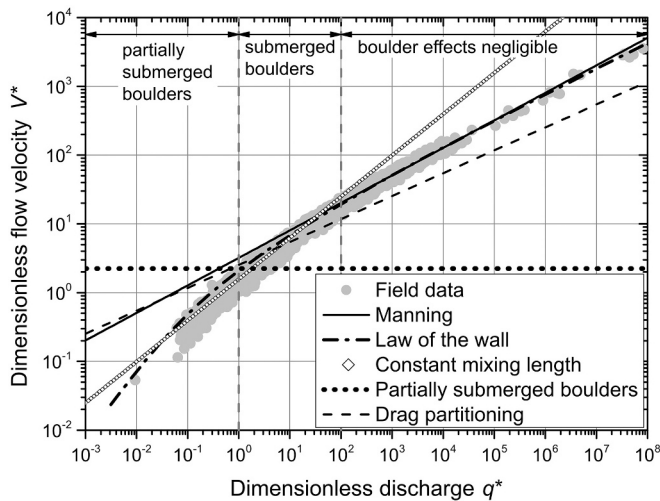


Fig. 7. Relationship between dimensionless discharge q^* and dimensionless flow velocity V^* for a field data compilation (grey dots; Rickenmann and Recking (2011)) of streams ranging from gravel to boulder beds. The Manning equation (black solid line; Eq. 6; Rickenmann and Recking (2011)) and the depth-integrated law of the wall (dash-dot; Eq. 7; Hey (1979)) were derived for boulder-free channels, corresponding to roughly $q^* > 100$. While the Manning equation does not fit boulder-rich channels well, the depth-integrated law of the wall fits surprisingly well across all three domains of relative roughness as noted by others (Ferguson, 2007). The constant mixing length model (white diamond; Eq. 8; Katul et al. (2002)) was developed for submerged boulders, corresponding to $1 < q^* < 100$, and fits well for $q^* < 100$ but does not work well in low roughness channels. Drag partitioning approaches have been suggested both for submerged (dashed; Eq. 9; Yager et al., 2007) and partially submerged boulders (dotted; Eq. 10; Lawrence (1997)). The constant dimensionless velocity (Lawrence, 1997) does not fit the data, while the drag-partitioning model for submerged boulders (Yager et al., 2007) begins to diverge from the data when boulders protrude above the flow. Calculations for the drag-partitioning model (Eq. 9; Yager et al. (2007)) were made using $C_{\text{boulder}} = 0.4$, $C_{\text{bed}} = 0.047$, $p/D_{84} = 0.5$, and $\Gamma = 0.5$.

where q is the volumetric water discharge per unit channel width. Note that the relative flow depth H/D_{84} is equal to q^*/V^* for a rectangular channel. The use of the two dimensionless variables collapses data compiled by Rickenmann and Recking (2011) from a wide range of field conditions onto a single curve (Fig. 7), with a maximum scatter of a factor of about 5 for a given value of q^* .

The velocity and discharge data (Fig. 7) can be classified into three commonly used q^* domains (e.g., Bathurst et al., 1981): negligible influence of boulders for $q^* > 100$ (small-scale roughness; $H/D_{84} > 7$), submerged boulders for $1 < q^* < 100$ (intermediate-scale roughness; $1 < H/D_{84} < 7$), and partially submerged boulders for $q^* < 1$ (large-scale roughness; $H/D_{84} < 1$).

Many common flow velocity equations can be expressed as a simple power function relating dimensionless velocity and discharge (Eqs. 4 and 5) such that

$$V^* = k_V q^{*a}, \quad (6)$$

where k_V is a dimensionless scaling parameter and a is a dimensionless constant. We discuss five commonly used flow velocity equations and assess their fit to field data across a wide range of relative roughness conditions (Fig. 7), with specific reference to boulder-induced high relative roughness conditions.

Two equations were derived for flows with negligible boulder effects ($q^* > 100$). The first, the Manning equation (Eq. 6 with values of $k_V = 3.2$ and $a = 0.4$, as determined empirically by Rickenmann and Recking (2011)), can be derived from the Kolmogorov (1941) phenomenological theory of turbulence (Gioia and Bombardelli, 2001), explicitly assuming that water depth is much larger than the relevant roughness size. It provides a good description of the data for $q^* > 100$, but not for boulder-rich, high-roughness channels (Fig. 7) (Rickenmann and Recking, 2011). The second, the law of the wall, is based on the Prandtl (1925) mixing length model under the assumption that the eddy mixing length scales with the height above the bed. It can be integrated to obtain a depth-averaged flow velocity (Keulegan, 1938; Hey, 1979). Making the explicit assumption that the flow depth is much larger than D_{84} , it yields

$$V^* = \left(\frac{\ln\left(\frac{q^*}{2V^*}\right) + 1}{\kappa} + B \right)^{2/3} q^{*1/3}. \quad (7)$$

Here, $\kappa = 0.44$ is von Karman's constant and B is a dimensionless constant equal to 9.5. Although Equation 7 was explicitly developed for boulder-free channels, it follows observations closely over the entire range of the data (Fig. 7). This is not the case if the aforementioned approximations are not made during the derivation.

For submerged boulders ($1 < q^* < 100$), two main approaches have been suggested. First, the mixing length model leading to the law of the wall has been adapted by using the assumption of a constant mixing length that scales with boulder size (Lawrence, 1997; Katul et al., 2002), yielding

$$V^* = \left(\frac{14}{15\kappa} \right)^{3/5} q^{*3/5}. \quad (8)$$

Although the scaling assumption lacks strong theoretical support and was essentially made *ad hoc*, the model provides a remarkably good fit to the data in the intermediate roughness range without any free parameters (Fig. 7). Second, some approaches use drag partitioning, summing over the drag forces of boulders and the boulder-free portion of the bed to predict reach-averaged velocity (e.g., Kean and Smith, 2006a, 2006b; Kean and Smith, 2010; Yager et al., 2007; Comiti et al., 2009). The physically-based model of Yager et al. (2007) is representative for this approach, and yields

$$V^* = \left(\frac{p}{D_{84}} \Gamma \frac{C_{\text{boulder}}}{2} + (1 - \Gamma) \frac{C_{\text{bed}}}{2} \right)^{-1/3} q^{*1/3}. \quad (9)$$

Here, C_{boulder} and C_{bed} are constant drag coefficients for the boulders

and the bed, respectively, p is the boulder protrusion into the flow, and Γ is the fraction of the channel bed covered with boulders. The approach yields a scaling exponent of 1/3, which is close to the observed scaling for boulder-free channels, but not for channels with submerged boulders (Fig. 7). Without additional assumptions—for example, non-constant drag coefficients—a different scaling cannot be obtained by classical drag partitioning approaches.

Finally, applying drag partitioning to partially submerged boulders ($q^* < 1$), Lawrence (1997) obtained a constant dimensionless flow velocity of the form

$$V^* = (\Gamma C_{\text{boulder}})^{-1/2}. \quad (10)$$

Equation 10, because it casts dimensionless velocity V^* as independent of dimensionless unit discharge q^* , captures neither the observed scaling nor the magnitude of the dimensionless flow velocity observed in the data (Fig. 7).

Summarizing, common approaches for estimating flow velocity like the Manning equation do not yield the correct velocity scaling in boulder-bed channels and should not be used for streams with substantial boulder roughness. The mixing length model for submerged boulders (Lawrence, 1997; Katul et al., 2002) gives a good fit to the data, but lacks strong theoretical support. Drag partitioning approaches, at least without the addition of further complexity, do not yield the observed scaling behavior. The integrated law of the wall (Eq. 7) follows the data over the entire range even though it was derived for boulder-free channels (Fig. 7). The good fit seems to be accidental, but the equation may be used as a comprehensive empirical approach. Theory-based equations that capture flow velocity scaling over the entire range of observations do not currently exist. However, empirical equations calibrated on a large data compilation have been put forward by Ferguson (2007) and Rickenmann and Recking (2011), and provide sufficient predictive power when no direct measurements are available but coverage of the full range of relative roughness values is needed (e.g., Nitsche et al., 2012).

4.2. Effects on sediment transport

The solid load of a river can be transported either in the water column as suspended load without frequent contact with the bed, or as bedload. Because suspended load is generally thought to be supply limited (e.g., Vanoni, 1975), it can be assumed that it is not greatly affected by the presence of boulders in the channel. In contrast, the reduced flow energy and increased roughness in boulder-bed channels need to be taken into account when making bedload transport predictions (e.g., Bathurst, 1987; Pagliara and Chiavaccini, 2006; Rickenmann, 2001; Yager et al., 2007; Papanicolaou et al., 2018).

Commonly used bedload equations, such as the Meyer-Peter and Müller (1948) equation, have been developed for streams with negligible boulder effects. Many bedload equations relate the dimensionless sediment transport rate (the Einstein number) q_s^* :

$$q_s^* = \frac{q_s}{\sqrt{g \left(\frac{\rho_s}{\rho} - 1 \right) D_{xx}^3}} \quad (11)$$

to the dimensionless shear stress (the Shields number) τ^* :

$$\tau^* = \frac{HS_r}{\left(\frac{\rho_s}{\rho} - 1 \right) D_{xx}} \quad (12)$$

Here, ρ_s and ρ are the densities of the sediment and the water, respectively, and D_{xx} is a representative grain size for the bedload sediment. A typical bedload equation takes the form (e.g., Meyer-Peter and Müller, 1948; Fernandez Luque and Van Beek, 1976)

$$q_s^* = K (\tau^* - \tau_c^*)^\alpha, \quad (13)$$

where K is the dimensionless transport efficiency, α is a

dimensionless constant, and τ_c^* is the critical Shields stress for the onset of bedload motion.

In principle, the presence of boulders can affect each of the four parameters on the right-hand side of the equation. The scaling exponent does not seem to strongly depend on the presence of boulders (e.g., Rickenmann, 2001). Several approaches account for form drag on immobile boulders by replacing the total Shields stress with a reduced effective stress that depends on bed slope or a measure of boulder size or roughness (e.g., Rickenmann, 2001; Pagliara and Chiavaccini, 2006; Rickenmann et al., 2006; Kean and Smith, 2006a; Yager et al., 2007, 2012; Kean and Smith, 2010). The critical Shields stress τ_c^* is known to increase with increasing channel bed slope (e.g., Lamb et al., 2008) due to increasing relative roughness at greater slopes (Prancevic and Lamb, 2015), which typically scales with the presence of boulders (e.g., Nitsche et al., 2011). Both of these effects reduce the driving stress responsible for transport relative to the transport threshold, and thereby reduce the transport rate (Fig. 8). Correction approaches based on these two physical effects yield similarly good results when compared to data (Schneider et al., 2015). The dimensionless transport efficiency K measures the unit effective Shields stress needed to transport a given amount of sediment. Conceptually, it can be thought of as a measure of the energy that is needed by the stream to transport a unit volume of sediment over a unit distance. In channels hosting large boulders, mobile bedload particles move slower and take a more tortuous path through the channel reach than they would in a boulder-free reach. This implies that transport efficiency decreases with increasing prevalence of boulders in the channel (e.g., Nitsche et al., 2011). Rickenmann (2001) showed that K is smaller than the values expected from common transport equations when the relative flow depth is smaller than $H/D_{84} \sim 7$ (see also Nitsche et al. (2011); Schneider et al. (2015)), a similar cutoff as observed for the effects of boulders on flow velocity (Fig. 7).

A number of approaches have been published to correct bedload transport rates for the presence of boulders (e.g., Pagliara and Chiavaccini, 2006; Rickenmann and Recking, 2011; Rickenmann et al., 2006; Yager et al., 2007). Nitsche et al. (2011) compared existing approaches to field data and concluded that the drag partitioning approach of Yager et al. (2007) yields the best match with observations. However, this

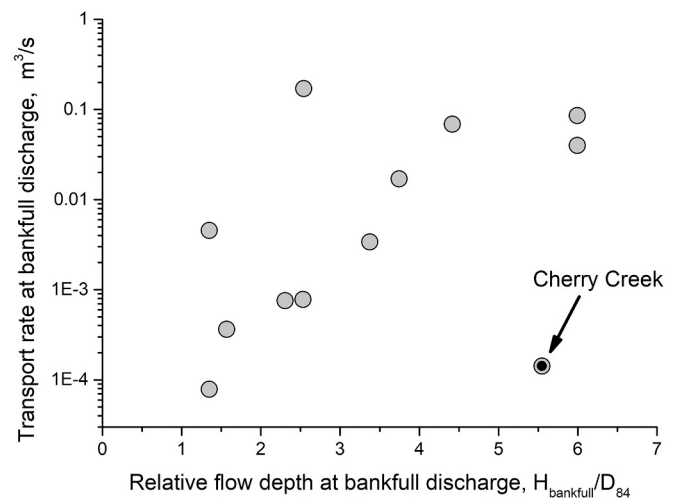


Fig. 8. Bedload transport rate at bankfull discharge as a function of the corresponding relative flow depth, defined as the ratio between bankfull flow depth and the representative grain size D_{84} , in the streams measured by Bunte and Swingle (2021) using bedload traps. This compilation includes streams mainly from the mountains of Colorado, USA, but also includes two sites in the Gros Venture Range, Wyoming, USA, and one site from the Cascade Range, OR, USA. All else equal, increased relative roughness due to the presence of boulders decreases bedload transport. At Cherry Creek (marked), flow depth was measured in a pool upstream of the sampling site where the flow is much deeper than at the location of the bedload traps.

approach requires values for parameters such as boulder size, spacing, and protrusion that are not usually measured. The correction approach of [Rickenmann and Recking \(2011\)](#) yielded the best result for cases where size, spacing, and protrusion values were unknown.

4.3. Effects on channel morphology

Channel morphology controls flow hydraulics and sediment transport, reflecting river adjustment to boundary conditions (e.g., [Yanites et al., 2010](#)) including the boulder supply from adjacent hillslopes (e.g., [Attal, 2017](#)). Boulders influence the efficiency of erosion processes and may impose erosion thresholds, or levels of erosive power below which substantial river erosion cannot occur due to boulder effects (e.g., [Seidl et al., 1994](#); [Johnson et al., 2009](#); [Scherler et al., 2017](#); [Shobe et al., 2018](#); [Raming and Whipple, 2020](#)). If the boulder supply remains consistent over channel adjustment timescales, rivers adjust to the hydraulic and bed cover effects of boulders by self-organizing their slope, width, and surface texture such that river incision can keep pace with baselevel fall ([Fig. 9](#)) ([Brocard and Van der Beek, 2006](#); [Johnson et al., 2009](#); [Attal, 2017](#)). Alluvial and bedrock channels represent two end-member channel states; both types of channels may adjust their geometry in response to the presence of boulders.

4.3.1. Alluvial rivers

In steep boulder-bed rivers, boulder delivery and transport cause reach-averaged channel steepening through the self-organization of the channel bed into cascade and step-pool morphologies ([Grant et al., 1990](#); [Montgomery and Buffington, 1997](#)). Cascade channels feature beds consisting of disorganized cobbles and boulders that dissipate flow energy due to tumbling and jet-and-wake flows ([Montgomery and](#)

[Buffington, 1997](#)). Step-pool channels exhibit pools, which often host deposited sediments, regularly alternating with channel-spanning steps formed by large clasts with dimensions that scale with the step height (e.g., [Curran and Wilcock, 2005](#)). Step-pool sequences are thought to be bedforms that evolve in a self-organizing process during extreme events ([Lenzi, 2001](#); [Turowski et al., 2009b](#); [Molnar et al., 2010](#)). Processes of step formation and destruction are governed by local hydraulics and channel morphology, and by granular processes (e.g., [Church and Zimmermann, 2007](#); [Curran, 2007](#); [Golly et al., 2019](#); [Zimmermann et al., 2010](#)). However, the mechanisms active in step-pool channel evolution (e.g., hydraulic, granular, and/or random control over step formation and destruction) and their relative importance are still debated (e.g., [Golly et al., 2019](#); [Saletti and Hassan, 2020](#)). Comprehensive reviews of step-pool channel processes and morphology have been given by [Chin and Wohl \(2005\)](#), [Church and Zimmermann \(2007\)](#), [Comiti and Mao \(2012\)](#), [Kalathil and Chandra \(2019\)](#), and [Zimmermann et al. \(2020\)](#). Even when flow hydraulics preclude the formation of step-pool bedforms, the presence of boulders in steep streams sets patterns of sediment erosion and deposition ([Monsalve and Yager, 2017](#); [Papanicolaou et al., 2018](#)) and determines the morphologic stability—or temporal consistency of channel morphology—of mountain streams (e.g., [Polvi, 2021](#)). Hillslope-derived boulders play a key role in the evolution of steep alluvial rivers by enhancing boundary roughness, driving channel steepening, and providing the keystones that form boulder and cobble bedforms like step-pool sequences ([Golly et al., 2017](#)).

There is increasing recognition that boulders may also play an important role in the evolution and form of gravel-bed rivers—as opposed to only boulder-bed, step-pool channels—beyond their long-recognized control on flow resistance (see summary by [MacKenzie et al. \(2018\)](#)). Because large grains anchor bed-stabilizing structures that

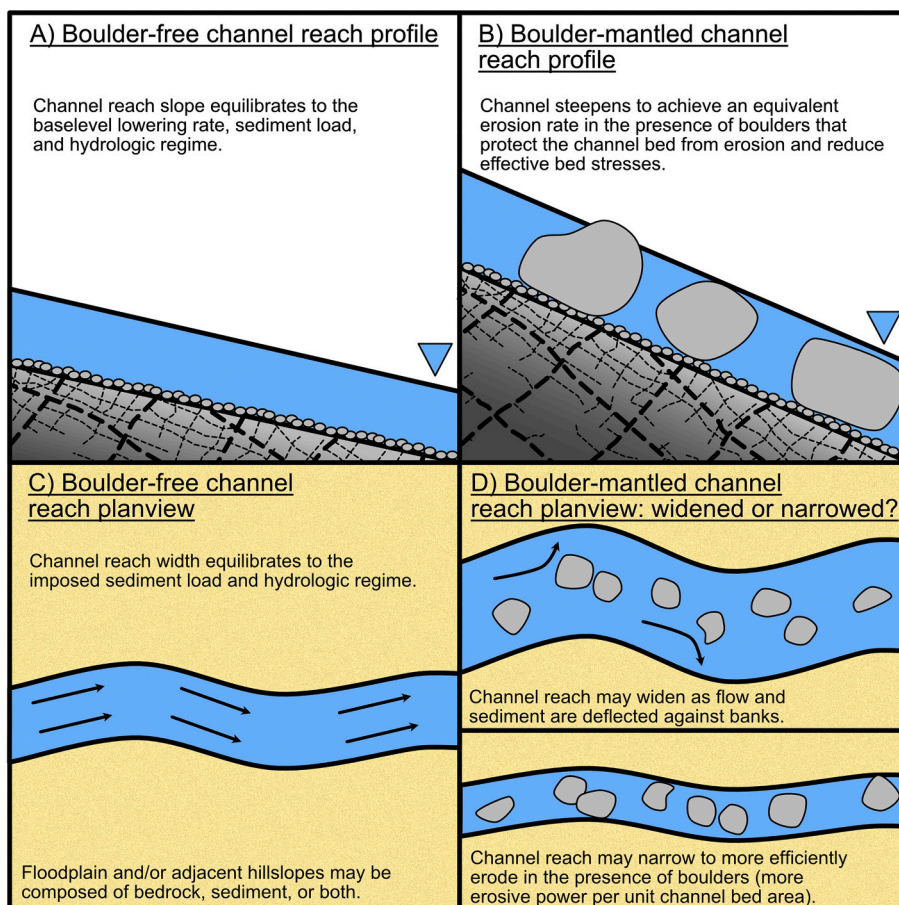


Fig. 9. Boulder effects on channel slope (A and B) and width (C and D). With all else equal, slope increases to achieve equilibrium with respect to the baselevel fall rate in the presence of boulders that cover the channel bed and reduce effective bed stresses. Channel width response to boulder delivery is less well understood. Channels may widen when boulder prevalence is high, possibly due to sediment-laden water being directed against the banks after encountering in-stream boulders. Alternatively, boulder delivery may cause channel narrowing that concentrates erosive power over a small channel bed area. The channel width response may hinge on factors not explored here such as bedload supply and transport dynamics or the relative resistance of boulders versus channel banks.

lead to immobile sediment patches and trapping of finer, otherwise-mobile grains (Laronne and Carson, 1976; Brayshaw et al., 1983; Hendrick et al., 2010; Papanicolaou et al., 2018), they may substantially reduce sediment transport rates for flows in which the largest grains remain immobile (Church et al., 1998; Booker and Eaton, 2020). This effect in turn is thought to significantly influence channel stability (MacKenzie et al., 2018).

In the end-member case where boulders are large enough to be immobile in the largest flows, alluvial channel morphology adjusts to the presence of boulders. Stream table experiments suggest that the largest grains stabilize channel banks, preventing lateral erosion at flows that mobilize most grains (MacKenzie and Eaton, 2017). Comparing experimental channels evolved using GSDs with widely differing D_{84} but identical D_{50} shows that channels with additional large grains steepen at discharges too low to mobilize the largest grains but achieve similar slopes at discharges that cause full mobility (Booker and Eaton, 2020). This indicates that the largest grains, when immobile, reduce the overall transport rate at a given slope, causing channel steepening. The morphologic stability of gravel-bed rivers may be set by the mobility of just a few large grains that remain less frequently mobile than the remainder of the grain-size distribution (Williams et al., 2019; Eaton et al., 2020). This idea is consistent with field analyses of fluvial channels whose planform evolution partially depends on the location and size of debris-flow-derived boulders (Whipple and Dunne, 1992). However, the finding that many gravel-bed rivers seem to have adjusted their shape to transport the D_{50} (Phillips and Jerolmack, 2016)—rather than a higher grain size percentile like the D_{84} —suggests the possibility that gravel-bed rivers with the highly disperse GSDs required for the largest grains to play an outsized role in setting channel form may be relatively rare.

4.3.2. Bedrock rivers

In channels incising bedrock, boulders reduce the erosive stresses exerted against the bedrock channel boundary. Boulder-induced hydraulic roughness reduces flow velocity (e.g., Schneider et al., 2015) and effective bed shear stress (e.g., Kean and Smith, 2006a; Yager et al., 2007). Immobile boulders act as persistent cover that inhibits incision into the bedrock surface (Thaler and Covington, 2016). Boulders may also disrupt sediment entrainment and reduce bedload transport rates (Section 4.2), thereby anchoring extensive areas of alluvial bed cover that extend beyond the boulders themselves (Nativ et al., 2019) and reducing the supply of erosive sediment “tools” (e.g., Sklar and Dietrich, 1998, 2004; Turowski et al., 2007). Bedrock channels must alter their morphology to erode at the rate of baselevel fall under their boulder supply conditions.

Assuming that river erosion is a function only of the shear stress exerted on the bedrock (i.e. that it does not explicitly depend on bed load sediment flux), the ratio of a boulder-mantled and a boulder-free channel slope S_{rb}/S_r can be derived as a function of boulder concentration, boulder size, and channel hydrology. Such an expression should include the effects of bed cover due to boulders, any differences in bed sediment size induced by the presence of boulders, and boulder-induced changes in flow resistance and form drag. An initial statement encompassing some of these effects can be made using the simplified model of Shobe et al. (2020) under the assumption that the slopes of boulder-mantled and boulder-free channels will adjust to equilibrate to the baselevel lowering rate and the presence of fully immobile boulders:

$$\frac{S_{rb}}{S_r} = \frac{(1 + \sigma_D)h_r}{(1 - \Gamma)h_{rb}} \quad (14)$$

Here, the subscript b denotes a parameter describing the boulder-mantled reach, h_r and h_{rb} are the flow depths in the boulder-free and boulder-mantled channel, respectively, and σ_D is the dimensionless drag stress exerted on the boulders (e.g., Kean and Smith, 2010). For a given erosion rate, the amount of boulder-induced steepening is expected to increase with the cover fraction of boulders and the drag stress, which is

a function of boulder size and spacing (Figs. 9A and B). This is conceptually consistent with findings comparing boulder size, bed cover, and channel steepness between channels with and without local supplies of boulders (Brocard and Van der Beek, 2006; Johnson et al., 2009; Thaler and Covington, 2016; Attal, 2017). The flow depths h_r and h_{rb} , the drag stress σ_D , and the cover fraction Γ all depend on boulder size and/or spacing such that numerical solutions to this equation are required (Shobe et al., 2020). Equation 14 is one starting point for connecting boulders to changes in steady-state channel slope, but such approaches need to be improved to account for other processes—like channel width adjustment and channel morphology changes due to bedload dynamics—that might be influenced by boulders.

Using equation 14 to describe boulder-induced channel steepening assumes that channel width does not adjust in response to boulder delivery or boulder-induced steepening (Shobe et al., 2020). The validity of this assumption has not been thoroughly assessed, as there have been few direct comparisons of channel geometry with boulder prevalence (Thaler and Covington, 2016; Finnegan et al., 2019; Nativ et al., 2019; Shobe et al., 2020) and inconsistent field evidence for the general relationships among channel width, slope, and erosion rate (e.g., Whipple, 2004; Duvall et al., 2004; Turowski et al., 2009a). Field data from northern California indicates that channel width (normalized for drainage area) decreases—albeit subtly and noisily—with increasing proximity to boulder-producing hillslope failures, suggesting that boulder delivery might reduce channel width (Shobe et al., 2020) (Figs. 9C and D). Other work in the same area, however, shows that narrowing due to hillslope-derived boulders may only occur in channels that are narrow relative to the seasonal displacement of boulder-delivering hillslope failures such that the potential for width adjustment may depend on the details of the boulder supply (Finnegan et al., 2019). The assumption of no width adjustment to boulder delivery may therefore be suspect (especially in cases of very rapid boulder supply (Finnegan et al., 2019)), but is subject to three important caveats. First, Shobe et al. (2020) did not directly correlate boulder prevalence with channel width, but instead used hillslope failure proximity as a proxy for boulder prevalence. Second, the observed correlation could have arisen from transient channel response to spatially variable rock uplift rates (e.g., Amos and Burbank, 2007; Lavé and Avouac, 2001) in their study area, which they lacked the data to constrain. Third, observed narrowing could be due not to boulder delivery but to the large amounts of transportable sediment delivered to the channel (e.g., Croissant et al., 2017), which has been shown to cause narrowing in other settings (e.g., Golly et al., 2017).

Other recent field results also suggest a role for channel width adjustment to boulder delivery, but imply a boulder-induced widening rather than narrowing (Figs. 9C and D). Studied reaches of the Liwu River, Taiwan, are in general wider when more boulders are present in the channel (Nativ et al., 2019). Building upon sediment-flux-dependent incision theory, Nativ et al. (2019) hypothesized that immobile boulders influence incision 1) by modifying bed cover dynamics and 2) by acting as additional channel boundaries, thus concentrating bedload tools on the exposed fraction of the bed. Boulders can also direct mobile bedload tools against channel banks (Fuller et al., 2016; Li et al., 2020) due to lateral deflection of bedload trajectories. Assuming, along similar lines to Shobe et al. (2020), that the channel has adjusted to the boulder supply, steady-state boulder-influenced reach width W_b can be cast as a power function of the bed cover fraction (Nativ et al., 2019):

$$\frac{W_b}{W} \propto (1 - \Gamma)^{-\gamma}, \quad (15)$$

where W is the width of a reach without immobile boulders and γ is a positive dimensionless constant. Equation 15 suggests that boulder-induced channel widening scales with the boulder bed cover fraction Γ . Currently, insufficient field data exists to thoroughly test the channel width response to boulder delivery, or to rule out the competing

possibilities that 1) boulders preferentially deposit in wider river reaches, or 2) bank failures that widen the channel also produce boulders (Marcotte et al., 2021). Width adjustment likely depends not only on boulder size and prevalence, but also on the relative erosion resistance of boulders and the channel banks as well as bedload transport dynamics.

Together, Equations 14 and 15 provide one possible framework for understanding how key channel morphologic variables (slope and width) adjust to sustained boulder delivery. Additional field studies are needed to 1) reconcile seemingly opposing field observations and account for climatic, lithologic, and other site-dependent controls on the interplay between boulder prevalence and channel geometry, and 2) better quantify the rates and processes of boulder delivery, transport, and degradation that set the in-channel boulder size distribution. It is also critical to separate transient channel responses to boulder delivery from the morphology exhibited by a boulder-influenced channel that is equilibrated to all of its forcing conditions including the boulder supply and the efficiency of boulder removal through fluvial transport and degradation.

4.4. Transport and degradation of boulders

The residence time of a boulder within a channel is limited by the river's ability to transport it and to reduce its size by wear. Boulder transport is difficult to study in the field because it tends to occur only during exceptional flow events (Carling and Tinkler, 1998; Cook et al., 2018; Turzewski et al., 2019; Huber et al., 2020), and because the assumptions underlying standard incipient motion calculations do not apply to the hydraulically rough, unsteady flows in which boulders often move (Carling et al., 2002; Alexander and Cooker, 2016). In the absence of fluvial power sufficient to transport boulders, they can gradually move by scouring of the surrounding sediment that then allows boulder rolling or toppling. Scour-caused boulder toppling events have been documented in the field (Yin and Shyu, 2017) and in experiments (Schlömer et al., 2021; Polvi, 2021). Repeated rolling or toppling periodically reorients boulders such that over time different facets of the boulders face upstream and thereby become vulnerable to abrasion (Wilson et al., 2013).

In steep landscapes, fluvial boulder transport can occur during exceptional events. In the intensively monitored Erlenbach in Switzerland, a large flood moved boulders up to 1.35 m in diameter (Turowski et al., 2009b), the largest of which weighed an estimated 2.5 tons. Catastrophic floods triggered by failures of glacial lakes and landslide dams can move boulders of over 10 m in diameter (Cook et al., 2018; Turzewski et al., 2019; Huber et al., 2020). Floods with rapidly increasing discharge such as glacial lake outburst floods or landslide-dam breach events cause boulder motion due to both unusually high discharge and rapid increases in flow velocity that generate large impulse forces and allow boulders to move even in cases where steady-flow calculations might suggest that no transport should occur (Alexander and Cooker, 2016). Abrupt, flood-driven reductions in the number and size of boulders in the channel immediately alter channel morphology and flow resistance (Golly et al., 2017); sediment fluxes may be elevated for several years following such exceptional events (Turowski et al., 2009b; Morche and Schmidt, 2012). This emphasizes the important role of boulders in stabilizing channels (e.g., Lenzi, 2002) during prolonged periods of immobility.

During periods without extreme events, immobile boulders are vulnerable to abrasion (e.g., Schumm and Stevens, 1973; Wilson et al., 2013) and chemical weathering (Seidl et al., 1994). We have only limited process-based theory and direct observations related to boulder abrasion, but insights from experiments and theory for pebble abrasion can be extrapolated. Abrasion is expected to occur when moving sediment particles collide with an immobile boulder, and is dominated by either attrition or fragmentation of mass (Attal and Lavé, 2009; Le Bouteiller et al., 2011). In field and experimental studies of pebble

abrasion, the abrasion rate depends strongly on lithology (Attal and Lavé, 2006), pebble traveling speed and initial size (Attal and Lavé, 2009). Fragmentation rates decrease during the experiments (Le Bouteiller et al., 2011), raising the possibility that large particles like boulders might have larger populations of pre-existing planes of weakness and may therefore be more prone to fragmentation (as opposed to abrasion) than the bedload fraction.

Immobile boulders are expected to erode by mechanisms similar to those governing *in situ* bedrock, and thus an analogy to bedrock incision can be made. Abrasion by mobile bedload on the exposed upstream faces of boulders, as well as on boulder sides and downstream faces in zones of fluid recirculation, likely drives boulder degradation in rivers with sufficient mobile bedload (Whipple et al., 2000; Wilson et al., 2013; Beer et al., 2017; Murphy et al., 2018). Plucking, the removal of fracture-bounded blocks, also occurs on boulder surfaces where planes of weakness are closely spaced (Whipple et al., 2000). As has been argued for channel floor bedrock (Hancock et al., 1998), plucking dominates in cases where boulders host closely spaced planes of weakness. In pervasively fractured rock, initial boulder production may exploit the fractures of greatest weakness with plucking of smaller blocks from in-channel boulders then occurring along remaining fracture planes.

4.5. Summary: Reach-scale effects of boulders in rivers

Immobile fluvial boulders increase hydraulic drag, reduce flow velocity and bedload transport, shield the channel bed from erosive stresses, and ultimately force rivers to adjust their geometry to achieve geologically dictated sediment transport and erosion rates. Channel steepening in response to boulder delivery has been consistently observed, but the response of channel width is not well constrained. The efficiency of boulder transport, and of the degradation processes that reduce boulder size and increase mobility, set the time-averaged boulder size distribution in eroding rivers under a given hillslope-derived boulder supply. The size distribution of boulders in turn controls how the channel adjusts to its baselevel fall rate and boulder supply boundary conditions. The river response to boulder delivery ultimately feeds back on adjacent hillslopes that respond to river erosion at their lower boundary, resulting in dynamic coupling between boulder-mantled channels and hillslopes.

5. Channel-hillslope coupling and boulder-influenced landscape evolution

How do boulder-mantled channels and hillslopes interact to set the long-term form and evolution of boulder-influenced landscapes?

Channels and hillslopes in eroding landscapes form a tightly coupled system (e.g., Harvey, 2001). Sediment delivery from hillslopes affects river erosion processes by setting the in-channel sediment availability and GSD. In turn, rivers set the lower boundary conditions to which hillslopes adjust. Rapid river incision leads to destabilization and accelerated erosion of hillslopes (Harvey, 2001; Larsen and Montgomery, 2012; Egholm et al., 2013; Golly et al., 2017; Campforts et al., 2020). The resulting influence of hillslope sediment delivery on river processes is known as downsystem coupling, while the influence of river erosion on hillslope evolution is upsystem coupling (Golly et al., 2017). Channel-hillslope coupling in boulder-rich landscapes is hypothesized to control landscape evolution at scales ranging from reach to basin.

At the channel reach scale, the erosion of previously stable boulder bedforms such as alluvial steps or boulder clusters can lead to an upstream-migrating pulse of river bed lowering that debuttresses adjacent hillslopes and (re-)activates landslide sediment supply to the channel. Golly et al. (2017) directly observed flood-driven upstream migration of an alluvial step, followed by landsliding and re-formation of a new step in approximately its original position. This cycle indicates both downsystem (landslide-derived coarse sediment influencing channel processes) and upsystem (debuttressing of hillslopes by

river erosion) coupling. Similarly, the degradation or transport of boulders protecting the channel bank from erosive stresses can lead to channel widening and increased landslide sediment delivery (Cook et al., 2018).

Modeling suggests that similar feedbacks govern the evolution of river valleys over geologic timescales on which direct observation is impossible (Fig. 10). Coupling a model for hillslope boulder production and transport (Glade et al., 2017) with a model for boulder-influenced bedrock rivers (Shobe et al., 2016) yields insight into how boulder delivery feedbacks between channels and hillslopes influence erosion in a river valley (Glade et al., 2019). A step change in baselevel lowering rate induces high-frequency (years to thousands of years) cycles in the vertical lowering rates of both the channel and the adjacent hillslopes. Initial rapid river erosion leads to hillslope steepening and enhanced boulder delivery to the channel. This then reduces river erosion rates due to boulder-induced bed cover and hydraulic drag. Boulder degradation and channel steepening enable a subsequent increase in river erosion rate that triggers accelerated hillslope erosion and causes the cycle to begin anew. These modeling results are analogous to the field observations of Golly et al. (2017) repeated over many cycles. The strength of both the downsystem and upsystem components of the coupling depends on boulder prevalence, size, and resistance to

degradation (Glade et al., 2019).

Even if direct observations of channel and hillslope processes at basin evolution timescales are elusive, both the downsystem and upsystem components of boulder-related channel-hillslope coupling have been observed at the landscape scale. Steep, rapidly eroding hillslopes can be destabilized by rapid river incision (the upsystem coupling) (e.g., Korup et al., 2010; Gallen et al., 2011; Attal et al., 2015). Resulting boulder delivery from hillslopes to channels results in large, in-channel boulder deposits that perturb channel longitudinal profiles, indicating that the boulders are influencing river erosion dynamics (the down-system coupling) (e.g., Korup, 2006; Korup et al., 2006; Ouimet et al., 2007; Finnegan et al., 2019).

Boulder delivery feedbacks between channels and hillslopes influence both the evolution of transient landscapes and the form of steady-state landscapes as the land surface adjusts simultaneously to its baselevel fall rate and the lithologically modulated boulder supply.

5.1. Transient adjustment of boulder-influenced landscapes

The size, prevalence, and erosion resistance of boulders in a landscape, while being influenced by external factors like rock type and fracture density, evolve during landscape response to a tectonic or climatic perturbation. Boulders have been said to inhibit landscape response to external (e.g. tectonic, climatic) forcing (Bennett et al., 2016; Shobe et al., 2016). While this is true relative to a hypothetical case in an identical landscape without boulders, it is more accurate to say that boulder dynamics are part of the landscape response to boundary conditions along with changes in channel and hillslope morphology. The influence of boulders on transient landscape evolution depends on the direction and magnitude of the forcing—for example, whether a landscape experiences an increase or decrease in baselevel fall rate or climate-induced erosivity. Boulder effects on transient landscape evolution have been best studied in regions undergoing accelerated baselevel fall (or rock uplift relative to baselevel) where an increase in erosion rate triggers river incision accompanied by channel-hillslope boulder delivery feedbacks (Bennett et al., 2016; DiBiase et al., 2018a; Finnegan et al., 2019).

As a drainage basin begins to respond to a baselevel perturbation, river erosion caused by the external forcing increases the erosion rate felt by adjacent hillslopes (e.g., Gallen et al., 2011). If the basin is underlain by rock types with amenable mineralogy and fracture density, boulder production and the rate of boulder delivery to the channel increase (Attal et al., 2015; Sklar et al., 2017). The baselevel fall rate may be fast enough to trigger hillslope destabilization and landsliding, which is the source of many of the in-channel boulder deposits reported in the literature (e.g., Korup, 2006; Ouimet et al., 2007; Bennett et al., 2016; Finnegan et al., 2019; Shobe et al., 2020). Even in the absence of landsliding, hillslopes may adjust by steepening and causing boulders to move downslope more rapidly than in the relict portion of the landscape (Glade et al., 2019). Accelerated boulder transport from hillslopes to channels results in boulders spending less time weathering and leading to greater in-channel boulder concentrations (Attal et al., 2015; Sklar et al., 2017).

The delivery of boulders in response to channel erosion forced by baselevel lowering then results in partial or complete inhibition of river erosion until the river adjusts to accommodate the erosion-inhibiting effects of boulders (Ahnert, 1987; Howard, 1998; Shobe et al., 2016; Glade et al., 2019). For riverbed incision rates to match the rate of baselevel fall in heavily boulder-mantled channels, boulders must be moved during large floods (Cook et al., 2018; Shobe et al., 2018), weathered and/or abraded in place with the river evacuating decay products (Prancevic et al., 2020), or moved as knickpoints in the underlying bedrock propagate upstream (Seidl et al., 1994; Howard, 1998; Finnegan et al., 2019). In the presence of sustained boulder supply, river channel slope and potentially width must adjust (see Section 4.3) to enable sufficient boulder transport and/or degradation such that erosion

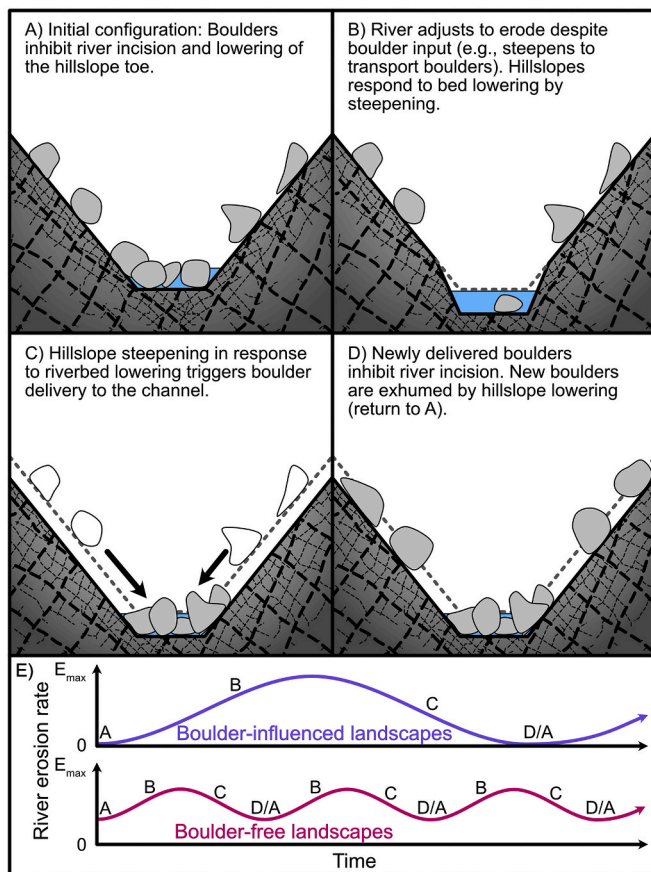


Fig. 10. The influence of boulder dynamics on channel-hillslope coupling. A–D show a repeating cycle of inhibition of erosion due to boulders (A), river adjustment to the supplied boulder load (B), renewed boulder delivery in response to river erosion (C), and a new phase of erosion inhibition by boulders (D). E) Time series of river erosion rates. The key effect of boulders, as opposed to more easily transportable hillslope-derived sediment (e.g., Croissant et al., 2017), is that boulders persist longer in the channel and therefore alter the timescales of channel-hillslope coupling cycles. Boulders may also increase the amplitude of river erosion rate cycles by more completely inhibiting erosion when boulders are present and forcing rivers to become highly erosive during periods when erosion can occur (Glade et al., 2019).

can proceed at the baselevel fall rate. Another possible mechanism of channel adjustment to boulder delivery is the formation of epigenetic gorges, in which channels do not incise boulder deposits but instead re-route and incise nearby bedrock (Ouimet et al., 2008; Johnson et al., 2009; Finnegan et al., 2019).

Boulder delivery to rivers through channel-hillslope coupling, relative to a case in which equivalent rock volume is supplied to the channel in more easily transported size classes, influences rates of transient signal propagation through drainage basins. The unsteady nature of boulder delivery to channels makes the upstream retreat of knickpoints episodic, with rapid propagation occurring during brief periods of increased erosive power and punctuated by periods of stasis during which high concentrations of in-channel boulders prevent channel adjustment. Support for boulder-induced unsteady signal propagation comes from field observations of channels where occasional large floods mobilize channel-defining boulders, allowing incision (Cook et al., 2018) and alluvial step retreat (Golly et al., 2017). One-dimensional channel profile modeling suggests that similar unsteadiness persists over geologic time purely due to boulder dynamics from channel-hillslope coupling (Shobe et al., 2016). In a scenario where hillslopes respond to river incision by delivering boulders, modeled knickpoint retreat rates become highly variable in time, varying by up to a factor of two around the mean. Long periods with little baselevel signal propagation occur while the channel adjusts its geometry to enable transport of hillslope-derived boulders and subsequent bed erosion. Brief periods of fast signal propagation then occur until boulder delivery triggered by rapid incision reduces the river erosion rate again.

Channel-hillslope coupling dynamics can alter landscape response to boundary conditions beyond pulses of baselevel fall; these include cessation of baselevel fall in post-orogenic landscapes (e.g., Mills, 1981, 1989) as well as climate change that might influence boulder production (e.g., Del Vecchio et al., 2018; Chilton and Spotila, 2020; Marshall et al., 2021).

5.2. Steady-state boulder-influenced landscapes

Boulder-influenced landscapes can only achieve steady state when tectonic or climatic fluctuations occur on timescales longer than those required for the landscape to fully adjust to its boundary conditions and boulder size distribution. Even in the presence of steady external forcings, boulder-mantled landscapes may never achieve true steady state due to the internal dynamics associated with channel-hillslope coupling. Numerical models accounting for channel-hillslope coupling in boulder-influenced landscapes suggest that channels and hillslopes achieve a time-averaged steady state if the averaging timescale is greater than the recurrence timescale of channel-hillslope feedback cycles (Shobe et al., 2016; Glade et al., 2019). Modeled erosion rates depart from the steady-state value over annual to millennial timescales due to 1) erosion inhibition by boulders newly delivered to a point on the landscape and 2) rapid erosion during periods when a landscape adjusted to the presence of boulders is boulder-free. Modeled steady-state, boulder-influenced channels and hillslopes are steeper than equivalent landforms without boulder delivery. Boulder influences on erosion and transport processes result in landscapes that must steepen to erode at the baselevel fall rate and transport all of the supplied sediment load in the presence of boulders.

Model predictions are conceptually consistent with field evidence from a recent field study from a set of near-steady-state mountain ranges with similar rock type and hydroclimate (DiBiase et al., 2018b). The two ranges differ primarily in bedrock fracture density, with lower fracture density yielding larger boulders (maximum grain sizes of 6 m versus 2 m). The range with prevalent boulders has steeper river channels, hillslopes, and higher total relief (DiBiase et al., 2018b).

Investigation of the long-term evolution of boulder-influenced landscapes has revealed the importance of boulders as agents of coupling between channels and hillslopes. Boulder-influenced

landscapes can achieve an average steady-state condition, but boulder dynamics dictate the rate and style of landscape adjustment to perturbations as well as the resulting steady-state landscape form.

5.3. Modeling long-term landscape evolution in the presence of channel-hillslope boulder feedbacks

Improved understanding of upsystem and downsystem channel-hillslope coupling due to boulder dynamics has led to attempts to integrate this behavior into large-scale landscape evolution models. Efforts have focused on using simple adjustments to widely used river incision models to incorporate the downsystem effects of hillslope-derived boulders on river erosion. Analogous approaches for the long-term evolution of boulder-influenced hillslopes have not been developed; more work remains to be done to incorporate both components of channel-hillslope coupling into long-term, large-scale models.

The generic stream power model, for rivers in which erosion is limited by the detachment rate of material from the channel bed, holds that vertical bed lowering per unit time $\frac{\partial z}{\partial t}$ is

$$\frac{\partial z}{\partial t} = -K_f(\omega - \omega_c), \quad (16)$$

an expression loosely derived from the physics of sediment transport (Eq. 13). K_f is an erosion constant, ω is an erosive stress or power (bed shear stress or unit stream power) generally calculated as a power function of bed slope and water discharge or its surrogate, drainage area, and ω_c is a critical power required to initiate erosion (e.g., Howard, 1994; Whipple and Tucker, 1999; Lague, 2014). In the simple case where K_f and ω_c are constants, and ω depends only on water discharge and bed slope, there is no mechanism by which this model can incorporate the dynamic coupling between river incision and the delivery of hillslope-derived boulders (Seidl et al., 1994). This limitation has motivated efforts to incorporate boulder effects into each of the three variables on the right hand side of Equation 16.

Approaches in which erosive power ω is modified to account for the hydraulic roughness of boulders (see section 4 above; Kean and Smith, 2006a; Yager et al., 2007) are the most physically based way to incorporate boulder effects into Equation 16. Such approaches have been used in reach-scale models of boulder-influenced river erosion (Shobe et al., 2016, 2018; Glade et al., 2019), but require spatially and temporally resolved knowledge of the in-channel boulder size distribution. They also require explicit flow resistance calculations to account for boulder-induced roughness. The calculation of ω as a power-law function of water discharge and slope can include consideration of flow resistance by varying the relevant exponents (see for example Whipple and Tucker (1999)), leaving open the possibility that this calculation could encompass boulder dynamics through empirical flow resistance approximations (section 4).

The erosional efficiency factor K_f can also be modified to account for the effects of hillslope-derived boulders, reflecting observations that immobile boulders mantle beds and reduce river erosion rates relative to the no-boulders case. Modifying K_f is equivalent to adding a bed cover factor $(1 - \Gamma)$ (Sklar and Dietrich, 1998, 2004) that reflects the average proportion of the bed covered by boulders (Shobe et al., 2016) or the average proportion of time the bed is mantled with immobile material (Ouimet et al., 2007).

The other approach to including boulders in simple channel evolution models is to vary the erosion threshold ω_c (e.g., Scherler et al., 2017; Shobe et al., 2018; Raming and Whipple, 2020) to account for boulder effects. ω_c might be the power required to mobilize a boulder if the bed cannot erode at all in the presence of the existing boulder cover. Otherwise, a boulder-influenced threshold represents the average reduction in erosion attributable to the presence of boulders in the channel much like the $(1 - \Gamma)$ term represents average boulder cover. ω_c might be expected to scale with the baselevel fall rate given that channel-hillslope coupling results in greater boulder delivery to

channels when rapid river erosion steepens adjacent hillslopes (Shobe et al., 2018), but such a simple scaling leaves out many of the spatio-temporal dynamics of channel-hillslope coupling such as the delay in the onset of boulder delivery experienced by upstream river reaches that baselevel signals are slow to reach. A more realistic model might be one in which ω_c scales with channel steepness (slope normalized by drainage area) (Scherler et al., 2017), reflecting empirical correlations between channel steepness and in-channel boulder prevalence (Attal et al., 2015). This connection is intuitively appealing as it is thought to reflect accelerated boulder delivery due to adjacent hillslope steepening. But it does not distinguish between boulder mantling of channels as a response to, versus a driver of, channel steepening.

The diversity of ways to model boulder-influenced landscapes reveals a tension familiar to geomorphologists: the more process-based approaches require data (e.g., boulder size distributions) that is not widely available over the required spatial and temporal scales, while heuristic modifications to model parameters are currently too general to offer field-testable predictions for landscape form. In the absence of computationally expensive and parameter-rich models that explicitly track the production, transport, and effects of boulders across landscapes (e.g., Glade et al., 2019), the key avenue for future progress is finding ways to connect field observations to long-term models of river and landscape evolution. Transforming model parameters like K_f and ω_c into state variables that depend on boulder delivery dynamics (Ouimet et al., 2007; Scherler et al., 2017; Shobe et al., 2018; Raming and Whipple, 2020) will require field calibration of empirical relationships between observable and calculable topographic metrics (e.g., hillslope gradient, local relief) and boulder influences on landscape evolution processes. Robust empiricisms connecting simple landscape metrics to boulder-induced reductions in erosive power ω would allow progress in the same direction. While most attention has focused on simplified models for boulder-rich channels, a parallel is needed for hillslopes. Field studies, physical experiments, and numerical modeling all have a role to play in informing models for landscape evolution over geologic time in the presence of boulder-induced channel-hillslope feedbacks.

5.4. Summary: Channel-hillslope coupling and boulder-influenced landscape evolution

Boulder delivery from hillslopes to channels changes rates and processes of river erosion, which then feeds back to affect the evolution of adjacent hillslopes. Channel-hillslope feedbacks induced by boulder delivery reduce—and introduce unsteadiness into—the upstream propagation rate of baselevel signals. While landscapes experiencing strong boulder-related channel-hillslope coupling can likely reach a time-averaged topographic steady state, they may also experience substantial spatial and temporal erosion rate variations due to cycles of boulder delivery, channel adjustment, and hillslope response. Landscape evolution modeling approaches that incorporate these feedbacks are being developed, but currently lack process-based foundations. Accurate prediction of boulder dynamics in eroding landscapes is not only scientifically important, but also has the potential to mitigate costly geohazards.

6. Boulders as a component of geomorphic hazards

How do boulders contribute to geomorphic hazards, and how might improved understanding of boulder dynamics be used for geohazard mitigation?

In addition to exerting a strong influence over the shaping of landscapes, boulders amplify geohazards in steep landscapes arising from catastrophic hillslope failures and/or large flood events. The largest boulders tend to travel farther downslope than the main failure mass during rockfall and rockslide events, thus setting the boundary of the area at risk (e.g., Hungr et al., 2005). Boulders mobilized in large hillslope failures can contribute to the formation of landslide dams (Dunning et al., 2006; Ouimet et al., 2007; Fan et al., 2020), destroy

structures and infrastructure, and block disaster response access routes (Kargel et al., 2016). Boulders in debris flows enhance damage to structures by magnifying flow impact forces relative to a flow without boulders (Kean et al., 2019). Boulders carried by debris flows can block culverts and other channel constrictions, leading to overbank flow and increases in the total inundation area (Kean et al., 2019). On entering the river channel network, boulders transported during high flows may cause further problems, for example by blocking hydropower station infrastructure.

Following a landslide or flood event, boulders are the most difficult component of the deposit to remove, thus delaying disaster response and recovery. In the 2018 Montecito debris flows in California, large boulders blocked roads and recovery routes; the only way to remove them was to use explosives to break them up (reported by the Los Angeles Times on January 17th, 2018). After the 2015 Gorkha and Dolakha earthquakes in Nepal, boulders of up to 6 m³ were observed along the Araniko highway blocking the road (Regmi et al., 2016) and delaying disaster response. In July 2016, a monsoon flash flood amplified by a landslide-dam-burst flood in the Upper Bhote Koshi entrained > 6 m boulders that jammed the sluice gates of intake to a hydropower station, causing \$110 million of damage and delaying power generation.

Despite the additional hazards that boulders add to mass-movement-influenced landscapes, the production and transport of boulders during landslide, rockfall, and debris flow events have not been consistently considered in geomorphic hazard assessments. Landslide hazard is quantified as the probability of a landslide of a given size occurring within a given area over a given period of time (Guzzetti et al., 2005). Probabilistic landslide hazard assessment starts with statistical analysis of landslide inventories mapped from satellite or aerial imagery, which yield a landslide size–frequency distribution for a specific landscape (e.g., Malamud et al., 2004; Bennett et al., 2012; Dini et al., 2020). To produce maps of landslide risk where detailed landslide inventories do not exist, landslide susceptibility is analyzed as a function of landscape attributes such as surficial and bedrock geology (e.g., Dahal et al., 2008), topographic gradient (e.g., Stanley and Kirschbaum, 2017), and distance from potential landslide triggers like active faults (e.g., Kritikos et al., 2015). More recently, time-varying factors such as damage to slopes incurred by previous earthquakes, termed earthquake preconditioning, have been shown to be important in statistical models of landslide susceptibility (e.g., Parker et al., 2015). Other features of landslides that may be combined into hazard assessments are the mobility of landslides (i.e., the runout distance of a failed mass relative to its fall height or volume), and connectivity with the river system and thus potential to trigger cascading hazards in the fluvial system downstream (e.g., Li et al., 2016). While several of the variables incorporated into current hazard assessments (e.g., geology, slope damage) may indirectly include boulder effects, quantifying boulder production and mobility as a component of geohazards is an opportunity for improving risk assessment.

Adding boulder dynamics to geomorphic hazard assessments is hampered by two main challenges: understanding the prevalence and size distribution of boulders produced in a hazard event, and understanding the mobility and potential travel paths of preexisting boulders. Achieving the former by extracting reliable grain size information over large areas is effort-intensive even given the wide availability of high-resolution imagery. A focus on finding topographic proxies for boulder size and prevalence—which will only come with improved understanding of the relationships between landscape form and boulder production (e.g., Chilton and Spotila, 2020; Neely and DiBiase, 2020; Marc et al., 2021)—would enable better prediction of the sizes of boulders available to be mobilized in a hazard event.

Even in locations with rich boulder size datasets, boulder mobility and transport dynamics are relatively poorly constrained (see sections 2 and 4). Recently, repeat high-resolution satellite imagery (Cook et al., 2018), imaging technologies including LiDAR and structure-from-motion from uncrewed aerial vehicles (Carr et al., 2020), and boulder

tracking approaches using GPS tags and accelerometers (section 6.1 below) have enabled field-based studies that investigate boulder mobility in geohazard-prone landscapes. Here we discuss a case study in which data from accelerometers embedded within boulders is used to assess boulder mobility in a landslide-hazard-prone area. While mobility data itself does not provide a full view of potential boulder-driven geohazards, assembling boulder mobility datasets is a key first step to understanding the influence of boulders on hazards in eroding landscapes.

6.1. Case study: Understanding boulder mobility with smart boulders

In a recent study, Dini et al. (2021) demonstrated the potential of smart boulders for monitoring a range of mass movement processes. Studies of boulder motion using *in situ* sensors can provide higher temporal resolution data on boulder mobility than can be achieved using traditional repeat surveying methods. The use of such sensors to understand boulder mobility in relation to geologic context and environmental forcing has the potential to 1) improve our mechanistic understanding of the controls on boulder incipient motion and travel pathways, and 2) provide a basis for geohazard early warning systems under the assumption that substantial boulder mobility preferentially occurs during catastrophic events in areas that are remote and difficult to monitor by other means. Because the size, prevalence, and transport dynamics of moving boulders influence the intensity of geohazards (Kean et al., 2019), tracking the motion—or lack thereof—of populations of boulders has implications for both basic science and geohazard mitigation.

Dini et al. (2021) equipped 23 boulders with GPS receivers to measure boulder position and accelerometers to measure boulder motion events. 10 boulders were embedded in a slow-moving landslide and the remainder in debris flow channels, which serves to capture boulder motion from two dominant transport mechanisms that may be

associated with geohazards. The boulders embedded in the landslide lie within the soil and might be expected to move coherently with the landslide mass if it were reactivated during intense rainfall events. Debris flow events may move boulders in the channels. The sensors used by Dini et al. (2021) can detect accelerations ranging from gradual boulder sliding and tilting to the $> 1g$ accelerations experienced by boulders entrained in debris flows.

Nine of the tagged boulders registered patterns in the accelerometer data compatible with downslope movements during the June–December 2019 observation period (Fig. 11). Of these, six lying within the landslide body show small angular changes, indicating a reactivation during the rainfall period and movement within the landslide mass. A qualitative validation, using images captured by a timelapse camera and repeat laser scans (Fig. 11), shows phases of reactivation and sliding of the mass. Three boulders, located in a debris flow channel, show sharp changes in orientation, likely corresponding to larger free movements and sudden rotations that may have occurred due to flow within the channel. Seismometer and timelapse camera data indicate a lack of large debris flows in the targeted channels during the 2019 monsoon season, in line with the accelerometer data showing few mobile boulders within the debris-flow channels. Dini et al. (2021) observed size-dependent boulder mobility in the channel; only the smallest boulders (< 2 m intermediate axis) moved during the acquisition season, likely due to the lack of substantial debris flows during the observation period. Boulders within the landslide did not show a size dependence, suggesting that boulders move coherently with the large landslide mass rather than independently based on their size. These findings lend tentative support to the idea that boulder transport on hillslopes is only size-dependent for some transport processes (Section 2), emphasizing the importance of quantifying the relative contributions of different transport processes (Section 2.3.3).

The field study of Dini et al. (2021) highlights the potential use of accelerometer-tagged boulders in hazard early warning systems, but

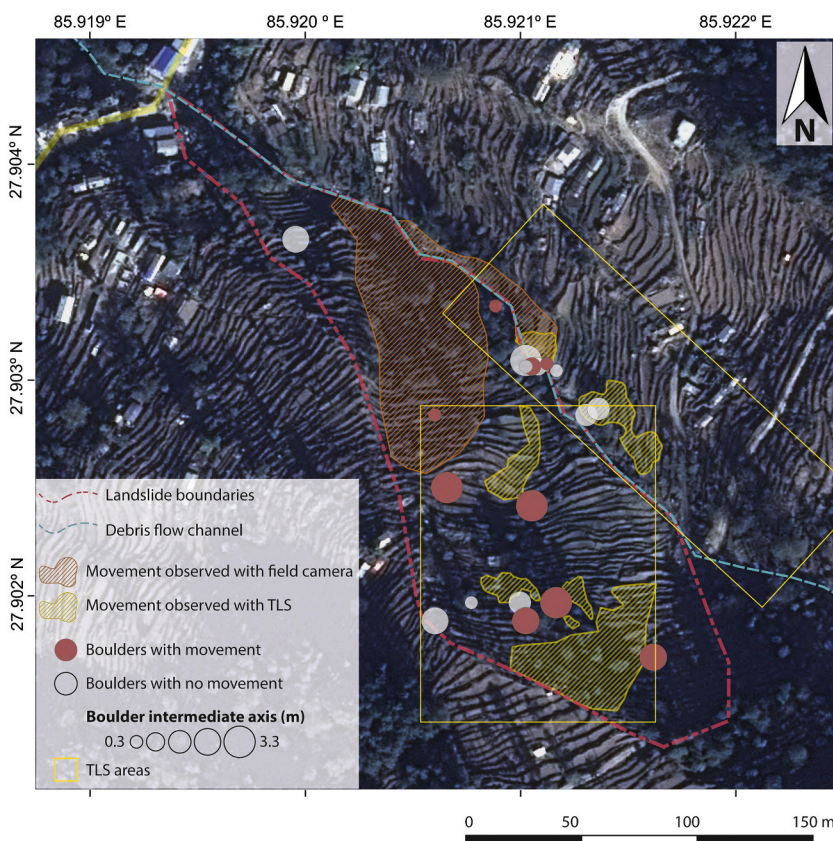


Fig. 11. Motion (or lack thereof) of boulders in Nepal tagged with accelerometers during a five month period (June–December 2019). The red dashed line delineates a landslide, portions of which moved during the observation period according to repeat field camera (located across the valley out of the map) and terrestrial laser scanner (TLS) data. The blue dashed line marks a debris flow channel. Nine tagged boulders moved—defined as experiencing accelerations or changes in angle above predefined thresholds—during the observation period. Boulder size as measured by intermediate axis length does not seem to exert a clear control over boulder (im) mobility within the landslide mass. The smallest boulders in the debris flow channel were the most mobile. Modified from Dini et al. (2021).

also points toward new ways of quantifying the drivers and modes of boulder mobility in general. By yielding high-resolution field datasets governing processes like boulder transport that are currently oversimplified in models (Shobe et al., 2016; Glade et al., 2017), field monitoring studies can simultaneously advance our understanding of landscape evolution and our ability to safeguard human lives and infrastructure from geohazards.

6.2. Summary: Boulders as a component of geomorphic hazards

Boulder transport during extreme geomorphic events adds to the hazards posed by those events (e.g., Hungr et al., 2005; Kean et al., 2019). Boulders in motion carry hazardous amounts of momentum and boulders that have come to rest are difficult to move. Improved understanding of boulder production and transport dynamics, using a combination of field sensors, repeat high-resolution measurements, and numerical models, will advance fundamental process understanding while enabling geohazard prediction and mitigation.

7. Synthesis and future directions

Boulders have long been hypothesized, based on intuition and qualitative field observations, to influence rates and processes of landscape evolution. Only recently have substantial numbers of studies attempted to quantify boulder effects on geomorphic processes and landscape evolution outcomes. We return to our guiding questions to summarize the current body of knowledge and assess specific needs for future research.

7.1. What factors control boulder production on eroding hillslopes and the subsequent downslope evolution of the boulder size distribution?

Boulders on hillslopes are produced by rockfall from exposed cliffs, landslides that access bedrock, or by weathering out of fractured bedrock as corestones. Boulder size, like the hillslope GSD in general, is a function of fracture density, rock type, climate, erosion rate, and the mechanism of boulder production. Boulder size and prevalence—though not necessarily residence time (Fig. 2)—increase in rapidly eroding landscapes where boulders are most likely to be produced by hillslope failures and most likely to bypass efficient weathering in the soil column, thereby reflecting bedrock fracture density.

The downslope boulder size distribution depends on the boulder production mechanism and subsequent transport and weathering. For example, rockfall from cliffs may preferentially deliver large boulders to the base of steep hillslopes while steady exhumation through the weathering zone might produce a more spatially uniform initial boulder size distribution (e.g., Fletcher and Brantley, 2010; Sklar et al., 2017). Size-dependent downslope transport can result in either downslope-fining or downslope-coarsening boulder size distributions depending on whether local or nonlocal transport dominates.

The size distribution of boulders on hillslopes—like the full GSD (Sklar et al., 2017)—is the combined result of production, transport, and weathering dynamics. A key avenue for future work on boulders specifically is to examine each set of processes in detail through well-constrained field observations, as we currently lack the ability to predict boulder size distributions from a process-based perspective. Boulder production may be best understood by mapping the boulder size distributions produced from recent or active production events such as rockfalls and landslides (e.g., Roda-Boluda et al., 2018; Finnegan et al., 2019; Shobe et al., 2020; Marc et al., 2021), or through detailed field monitoring using sediment fences (e.g., Rengers et al., 2020) and other site-scale techniques. Measuring *in situ* bedrock fracture density can yield estimates of the largest boulder that can be produced in a given landscape (Verdian et al., 2020; Neely and DiBiase, 2020). The use of high-resolution imagery (e.g., Neely and DiBiase, 2020) to collect large boulder size datasets across rock type, tectonic, and climatic gradients

will allow the formulation and testing of mechanistic boulder production models. *In situ* boulder-tracking (e.g., Dini et al., 2021) can isolate the influence of boulder transport on the downslope boulder size distribution. More studies using similar *in situ* methods or repeat high-resolution surveys (e.g., Carr et al., 2020) will enable the quantification of typical recurrence timescales and displacements associated with boulder motion. Weathering may be the most challenging control on the boulder size distribution to quantify, but initial steps have been made by using field instrumentation to record weathering processes (Eppes et al., 2010; Lamp et al., 2017; Eppes et al., 2020). Importantly, field observations of production, transport, and weathering must be compared across gradients of climate, lithology, and erosion rate to establish the relative effects of each variable on the downslope distribution of boulder sizes on hillslopes.

7.2. How do boulders influence hillslope processes and long-term hillslope evolution?

On hillslopes experiencing predominantly local sediment transport, boulders affect the processes of soil production and transport that govern hillslope evolution (Fig. 4 and 5). Relative to a hillslope of identical morphology without boulders, boulder-mantled hillslopes experience reduced soil production and transport rates due to boulders shielding the underlying hillslope from weathering agents and acting as obstacles to soil transport. The downslope distribution of boulder sizes determines the relative importance of boulder effects at each point on the hillslope and the magnitude of the morphologic response, leading to a wide range of possible hillslope morphologies (Fig. 6).

Hillslopes dominated by local transport adjust their form to accommodate the baselevel fall rate and boulder size distribution such that their slope at every point can be thought of as the sum of a soil transport component and a boulder-induced component (Eq. 3). In simple models informed by field data, the downslope boulder size distribution can drive hillslope adjustment to a convex-up, concave-up, or linear shape depending on how boulder size and spacing change with distance downslope (Fig. 6). The strong dependence of modeled hillslope form on the boulder size distribution emphasizes the importance of boulder production, transport, and weathering processes to the long-term shape of hillslopes. Future work may better characterize feedbacks between boulders and granular soil creep and flow processes (e.g., BenDror and Goren, 2018; Ferdowsi et al., 2018; Deshpande et al., 2020), changing expectations for the form and evolution of boulder-mantled hillslopes.

On steep, planar hillslopes dominated by nonlocal transport and near the threshold for mass-wasting, boulders are efficiently delivered to the hillslope toe and there exists no documented dependence of hillslope form on boulder size. Hillslope form is set by the erosion rate at the hillslope toe, which determines whether the hillslope will steepen enough to achieve its threshold angle, as well as the threshold angle itself which is governed by rock strength. Boulders delivered to the hillslope toe may ultimately influence hillslope boundary conditions through their influence on erosion processes in colluvial and fluvial channels.

There remains a need for data at the process scale detailing how boulders influence hillslope processes. While the damming effects of boulders on soil transport are relatively well-documented, the effects of boulders on weathering and soil production are not. Comparing weathering and soil production dynamics between otherwise similar, boulder-mantled and boulder-free hillslopes will advance our understanding of the specific mechanisms by which infrequently mobile boulders change weathering processes and resulting hillslope form. Even the question of whether substantial weathering can occur beneath stationary boulders, or whether weathering mainly occurs during periods without boulder cover, remains open.

Links between the downslope boulder size distribution and the form of hillslopes—both as a function of erosion rate (e.g., Neely et al., 2019; Neely and DiBiase, 2020) and climate and rock type (e.g., Verdian et al.,

2020)—need to be quantified in the field. This effort will be complicated by the need to determine whether a hillslope is in approximate steady state with respect to its erosion rate forcing, but cases where steady state is a reasonable assumption will yield insights into the control of the boulder size distribution on hillslope topography and its importance relative to external forcings.

7.3. How do boulders influence fluvial processes and river channel shape?

Boulders that remain largely immobile in river channels increase hydraulic drag and prevent erosive flows from accessing some portion of the channel bed. They reduce flow velocity (Fig. 7), effective bed shear stresses, and rates of bedload sediment transport (Fig. 8) relative to a boulder-free channel. Empirical corrections exist to adjust both flow resistance and bedload transport calculations for the presence of boulders, but more process-based approaches await development.

Channels adjust to the presence of large, immobile boulders by adjusting their cross-section shape and slope (Fig. 9). The slope of both alluvial and bedrock channels, all else equal, scales with boulder size and prevalence. The channel width response to boulder delivery is less clear, with evidence from some landscapes showing a positive correlation between boulder prevalence and channel width (e.g., Nativ et al., 2019), and some showing a decrease in width with increasing proximity to boulder-delivering landslides (Shobe et al., 2020). The widening response fits with the idea that boulders might deflect particle-laden flows against channel banks (e.g., Fuller et al., 2016; Li et al., 2020), but direct observations of this effect are lacking. More work is needed to clarify boulder-related influences on channel width independent of other controls on channel width like the narrowing caused by an increased flux of transportable sediment to the channel (Golly et al., 2017).

Fluvial boulders in some field sites show substantial abrasion, implying a long-residence time in a fixed orientation within the channel and suggesting that the largest boulders degrade in place through fluvial processes and weathering (Wilson et al., 2013). On the other hand, exceptionally large flow events move boulders over 10 m in diameter, suggesting an important role for transport as well. Mobilization of the largest boulders leads to extensive changes in channel geometry and sediment flux (Golly et al., 2017; Cook et al., 2018), emphasizing both that boulders strongly influence channel bed configuration and that such transport events must be relatively rare.

A key open question in boulder-influenced rivers is: how do boulder-mantled channels keep up with baselevel fall rates when there exists a consistent supply of seemingly immobile boulders? Collecting field data to understand the relative contributions of channel geometry adjustment, *in situ* boulder degradation (e.g., Schumm and Stevens, 1973; Wilson et al., 2013; Prancevic et al., 2020), and boulder transport during extreme events (e.g., Cook et al., 2018; Huber et al., 2020; Greenbaum et al., 2020) is important to answering this question. Repeat high-resolution field surveys will help determine which processes allow continued erosion in the presence of boulders, and how process dominance might change based on tectonic, climatic, and lithologic conditions.

7.4. How do boulder-mantled channels and hillslopes interact to set the long-term form and evolution of boulder-influenced landscapes?

Boulder delivery from hillslopes to channels is one manifestation of channel-hillslope coupling that results in both downsystem (hillslope-derived boulders influence river processes) and upsystem (river erosion dynamics set the lower boundary condition for hillslopes) effects (Fig. 10). Both components of this coupling have been observed over short timescales in the field (Golly et al., 2017) and replicated in numerical simulations (Glade et al., 2019). Boulder-related channel-hillslope coupling changes the upstream propagation of baselevel signals through drainage basins because of the time required for 1) channels to

adjust to boulder delivery and 2) hillslopes to respond to incision at their lower boundary. Simulations predict that, because of these time lags, transient landscape adjustment proceeds at unsteady rates in boulder-mantled landscapes (Shobe et al., 2016). In landscapes experiencing time-averaged steady-state erosion conditions, channel-hillslope coupling may continue to produce variations in channel and hillslope erosion rates through time (Glade et al., 2019). Boulder effects on these couplings, and on the amplitude and frequency of erosion rate fluctuations, are hypothesized to depend on boulder size, prevalence, and resistance to erosion.

The influence of boulders on landscape form and evolution will be best quantified by finding well-constrained field studies where long-term erosion rates can be measured with cosmogenic isotopes, and where boulder-rich portions of the landscape can be directly compared against boulder-poor portions (e.g., Thaler and Covington, 2016; DiBiase et al., 2018b,a). One challenge worth noting is that boulders themselves, unlike sand and gravel fractions, self-shield from cosmic rays and therefore can't be directly sampled and compared with other size fractions (e.g., Tofelde et al., 2018). However, cosmogenic surface exposure ages can constrain the "emplacement age" of boulders in the landscape if post-deposition mobility can be neglected (Huber et al., 2020).

The importance and timescales of up- and down-system channel-hillslope coupling due to boulder dynamics can be explored independently in the field by investigating river response to recent boulder delivery (Finnegan et al., 2019) or hillslope response to river-induced destabilization (Golly et al., 2017; Cook et al., 2018). Numerical models incorporating boulder effects on channel-hillslope coupling will need to better account for known feedbacks. For example, current models often incorporate the down-system effects of hillslope-imposed grain size variations on rivers (Egholm et al., 2013) without including up-system effects on hillslope grain size, or do so in a heuristic way (Glade et al., 2019). Physical landscape experiments represent another promising path towards understanding boulder-influenced landscapes through the lens of channel-hillslope coupling (Hasbargen and Paola, 2000; Bigi et al., 2006) if realistic ways of producing boulders in eroding experimental landscapes can be found.

7.5. How do boulders contribute to geomorphic hazards, and how might improved understanding of boulder dynamics be used for geohazard mitigation?

The presence of boulders enhances the risk associated with geohazards in eroding landscapes, including landslides, debris flows, and floods. Mobile boulders can destroy infrastructure and be challenging to remove due to their size, resulting in socioeconomic harm that persists long after a disaster event. Conversely, because the presence of boulders can slow water flow, erosion, and sediment transport, immobile boulders are often used in engineering projects that seek to mitigate erosion (e.g., Lenzi, 2002; Pagliara and Chiavaccini, 2006; Chin et al., 2009) and accompanying hazards (for example, streambank collapse). Prediction and mitigation of geohazards in either case requires explicit consideration of the likelihood that a given event will produce and/or mobilize boulders.

Known hazard areas can be intensively monitored using repeat high-resolution imagery and *in situ* boulder-tracking (Fig. 11). These approaches hold the promise of potential application to early warning systems, and will help constrain our process-based understanding of boulder production and movement through the landscape. Using rich field datasets to inform new numerical models for boulder dynamics in hazard-prone landscapes will enable *a priori* assessment of potential boulder-related hazards before extreme events occur.

8. Conclusions

The presence of infrequently mobile boulders influences the form

and evolution of nonglaciated, erosional landscapes. Dominant processes of boulder production—including landsliding, rockfall, and corestone exhumation—reflect external controls like rock type and fracture density as well as internal controls like erosion rate and landscape steepness. Boulders that persist on hillslopes inhibit soil production and transport, affecting hillslope shape in ways that depend on the dominant mode of sediment transport. When transport is predominantly local, hillslopes preferentially steepen in locations with larger or more closely spaced boulders. Depending on the downslope distribution of boulder size and spacing, hillslopes may achieve concave-up, linear, or convex-up steady-state shapes. Boulder effects are therefore likely encoded in the steady-state form of hillslopes not completely dominated by nonlocal transport. Boulders are more likely to bypass the hillslope without influencing hillslope form when nonlocal transport dominates, emphasizing that the steepest, fastest-eroding landscapes may not be those that experience the greatest boulder influence.

Boulder delivery from hillslopes to river channels drives increased hydraulic roughness and reduced bedload transport efficiency. Field-validated approaches exist to account for both effects, and suggest that channel geometry must adjust to allow erosion at the rate of baselevel fall despite boulder-induced reductions in erosion and transport efficiency. Reach-scale theory, experiments, and field observations agree that boulder delivery drives channel steepening to enable erosion to keep pace with baselevel fall, but the effects of boulders on channel width are less clear.

Feedbacks between boulder-influenced channels and hillslopes affect long-term landscape evolution trajectories, increasing the time required for landscapes to adjust to external perturbations and altering baselevel signals as they travel through drainage basins. The timescales over which boulder-influenced landscapes can be considered to be in steady state may need to be several orders of magnitude longer than for boulder-free landscapes, as channel-hillslope boulder delivery feedbacks cause cycles of internal disequilibrium unrelated to variations in tectonics, climate, or other external forcings. Boulder-influenced landscapes can nevertheless achieve a time-averaged steady-state form with hillslopes and channels that adjust their steepness—and potentially

other less-studied properties like hillslope soil thickness and river channel width—in response to boulder size and prevalence.

Boulders contribute to geomorphic hazards through their destructive power when mobile and their persistence in the landscape once they come to rest. The contribution of boulders to recent hazard events, coupled with results from field monitoring studies, indicates that explicit incorporation of boulder production and transport dynamics into geomorphic hazard assessment will improve hazard prediction and mitigation efforts.

Boulder dynamics are best thought of as one facet of a landscape's response to external environmental forcings, whether that forcing is a sustained acceleration in the baselevel lowering rate, the cessation of orogenic activity, or climatic changes that modulate the boulder supply. Key knowledge gaps stem from a lack of data on the processes that govern boulder size and prevalence, as well as how process-scale effects of boulders add up to influence landscape form and dynamics over time. Future work should prioritize field studies that treat boulder processes as one component of self-organizing landscapes, elucidate how boulder dynamics interact with other geomorphic processes, and quantify how boundary conditions like tectonics, climate, and rock type affect the balance of those interactions.

Declaration of Competing Interest

None.

Acknowledgements

New data collected for this study is available in a public repository (Shobe et al., 2021). C.M. Shobe was supported by H2020 Marie Skłodowska-Curie Actions grant no. 833132 (STRATASCAPE). R.C. Glade and C.M. Shobe thank Bob Anderson and Greg Tucker for five years of guidance on the boulder problem. We thank Kristin Bunte and Dieter Rickenmann for providing data on bedload transport rates and flow velocity. Mikael Attal, one anonymous reviewer, and Editor Alessandra Negri gave thorough and constructive reviews.

Appendix A. Notation table

Symbol	Units	Meaning
a	-	Discharge–velocity exponent
B	-	Dimensionless constant
C_{boulder}	-	Boulder drag coefficient
C_{bed}	-	Bed drag coefficient
D	L	Hillslope boulder size
D_{xx}	L	Representative grain size for fluvial bedload
D_{84}	L	Size of the 84th percentile of bed sediment
g	L ² /T	Acceleration due to gravity
H	L	Flow depth
H_{bankfull}	L	Bankfull flow depth
h_r	L	Flow depth in boulder-free reach
h_{rb}	L	Flow depth in boulder-mantled reach
k	L ² /T	Soil transport efficiency
K	-	Bedload transport efficiency
K_f	varies	Fluvial erosion efficiency
k_v	-	Discharge–velocity coefficient
L	L	Boulder spacing
p	L	Boulder protrusion height
q_{soil}	L ² /T	Hillslope soil flux per unit width
q	L ² /T	Specific water discharge
q^*	-	Dimensionless water discharge
q_s^*	-	Dimensionless bedload transport rate
q_s	L ² /T	Volumetric bedload transport rate
S_h	-	Hillslope topographic gradient
S_r	-	Riverbed topographic gradient
S_{rb}	-	Slope of a boulder-mantled channel
t	T	Time

(continued on next page)

(continued)

Symbol	Units	Meaning
V	L/T	Reach-averaged flow velocity
V^*	-	Dimensionless reach-averaged flow velocity
w	L/T	Hillslope weathering rate
W	L	Boulder-free channel width
W_b	L	Boulder-mantled channel width
x	L	Distance
z	L	Topographic elevation
α	-	Bedload transport onstant
γ	-	Channel width constant
Γ	-	Fraction of the channel bed covered by boulders
κ	-	Von Karman's constant
ρ_s	M/L ³	Sediment density
ρ	M/L ³	Water density
σ_D	-	Dimensionless drag stress on in-channel boulders
τ^*	-	Shields stress
τ_c^*	-	Critical Shields stress
ω	varies	Fluvial erosive power
ω_c	varies	Critical fluvial erosive power

References

- Ahnert, F., 1987. Process-response models of denudation at different spatial scales. *Catena*. Supplement (Giessen) 10, 31–50.
- Aldred, J., Eppes, M.C., Aquino, K., Deal, R., Garbini, J., Swami, S., Tuttle, A., Xanthos, G., 2016. The influence of solar-induced thermal stresses on the mechanical weathering of rocks in humid mid-latitudes. *Earth Surf. Process. Landf.* 41, 603–614.
- Alexander, J., Cooker, M.J., 2016. Moving boulders in flash floods and estimating flow conditions using boulders in ancient deposits. *Sedimentology* 63, 1582–1595.
- Amos, C.B., Burbank, D.W., 2007. Channel width response to differential uplift. *J. Geophys. Res. Earth Surf.* 112.
- Anderson, R.S., 1998. Near-surface thermal profiles in alpine bedrock: Implications for the frost weathering of rock. *Arct. Alp. Res.* 30, 362–372.
- Anderson, R.S., 2014. Evolution of lumpy glacial landscapes. *Geology* 42, 679–682.
- Andrews, D., Bucknam, R.C., 1987. Fitting degradation of shoreline scarps by a nonlinear diffusion model. *J. Geophys. Res. Solid Earth* 92, 12857–12867.
- Ashworth, P.J., Ferguson, R.L., 1989. Size-selective entrainment of bed load in gravel bed streams. *Water Resour. Res.* 25, 627–634.
- Attal, M., 2017. Linkage between sediment transport and supply in mountain rivers. *Gravel-Bed Rivers* 329–353.
- Attal, M., Lavé, J., 2006. Changes of bedload characteristics along the marsyandi river (central nepal): Implications for understanding hillslope sediment supply, sediment load evolution along fluvial networks, and denudation in active orogenic belts. *Geol. Soc. Am. Spec. Pap.* 398, 143–171.
- Attal, M., Lavé, J., 2009. Pebble abrasion during fluvial transport: Experimental results and implications for the evolution of the sediment load along rivers. *J. Geophys. Res. Earth Surf.* 114.
- Attal, M., Mudd, S., Hurst, M., Weinman, B., Yoo, K., Naylor, M., 2015. Impact of change in erosion rate and landscape steepness on hillslope and fluvial sediments grain size in the feather river basin (sierra nevada, california). *Earth Surface Dynam.* 3, 201–222.
- Balco, G., Finnegan, N., Gendaszek, A., Stone, J.O., Thompson, N., 2013. Erosional response to northward-propagating crustal thickening in the coastal ranges of the us pacific northwest. *Am. J. Sci.* 313, 790–806.
- Bathurst, J.C., 1978. Flow resistance of large-scale roughness. *J. Hydraul. Div.* 104, 1587–1603.
- Bathurst, J., 1987. Bed load discharge equations for steep mountain rivers. In: *Sediment Transport in Gravel-Bed Rivers*, pp. 453–491.
- Bathurst, J.C., Simons, D.B., Li, R.M., 1981. Resistance equation for large-scale roughness. *J. Hydraul. Div.* 107, 1593–1613.
- Beatty, C.B., 1989. Great big boulders i have known. *Geology* 17, 349–352.
- Beer, A.R., Turowski, J.M., Kirchner, J.W., 2017. Spatial patterns of erosion in a bedrock gorge. *J. Geophys. Res. Earth Surf.* 122, 191–214.
- Beeson, H.W., McCoy, S.W., Keen-Zebert, A., 2017. Geometric disequilibrium of river basins produces long-lived transient landscapes. *Earth Planet. Sci. Lett.* 475, 34–43.
- BenDror, E., Goren, L., 2018. Controls over sediment flux along soil-mantled hillslopes: Insights from granular dynamics simulations. *J. Geophys. Res. Earth Surf.* 123, 924–944.
- Bennett, G., Molnar, P., Eisenbeiss, H., McArdell, B., 2012. Erosional power in the swiss alps: characterization of slope failure in the illgraben. *Earth Surf. Process. Landf.* 37, 1627–1640.
- Bennett, G.L., Miller, S.R., Roering, J.J., Schmidt, D.A., 2016. Landslides, threshold slopes, and the survival of relict terrain in the wake of the mendocino triple junction. *Geology* 44, 363–366.
- Bigi, A., Hasbargen, L.E., Montanari, A., Paola, C., et al., 2006. Knickpoints and hillslope failures: Interactions in a steady-state experimental landscape. *Special Papers Geol. Soc. America* 398, 295.
- Birkeland, P.W., 1968. Mean velocities and boulder transport during tahoe-age floods of the truckee river, california-nevada. *Geol. Soc. Am. Bull.* 79, 137–142.
- Blair, T.C., McPherson, J.G., 1999. Grain-size and textural classification of coarse sedimentary particles. *J. Sediment. Res.* 69, 6–19.
- Bones, J., 1973. Process and sediment size arrangement on high arctic talus, southwest devon island, nwt, canada. *Arct. Alp. Res.* 5, 29–40.
- Booker, W.H., Eaton, B.C., 2020. Stabilising large grains in self-forming steep channels. *Earth Surface Dynam.* 8, 51–67.
- Bourrier, F., Dorren, L., Nicot, F., Berger, F., Darve, F., 2009. Toward objective rockfall trajectory simulation using a stochastic impact model. *Geomorphology* 110, 68–79.
- Brayshaw, A.C., Frostick, L.E., Reid, I., 1983. The hydrodynamics of particle clusters and sediment entrapment in coarse alluvial channels. *Sedimentology* 30, 137–143.
- Brocard, G., Van der Beek, P., 2006. Influence of incision rate, rock strength, and bedload supply on bedrock river gradients and valley-flat widths: Field-based evidence and calibrations from western alpine rivers (southeast france). In: Willett, S.D., et al. (Eds.), *Spec. Pap. Geol. Soc. Am.* 398, pp. 101–126.
- Brocard, G.Y., Willenbring, J.K., Miller, T.E., Scatena, F.N., 2016. Relict landscape resistance to dissection by upstream migrating knickpoints. *J. Geophys. Res. Earth Surf.* 121, 1182–1203.
- Bruthans, J., Soukup, J., Vaculikova, J., Filippi, M., Schweigstillova, J., Mayo, A.L., Masin, D., Kletetschka, G., Rihosek, J., 2014. Sandstone landforms shaped by negative feedback between stress and erosion. *Nat. Geosci.* 7, 597–601.
- Bunte, K., Poesen, J., 1993. Effects of rock fragment covers on erosion and transport of noncohesive sediment by shallow overland flow. *Water Resour. Res.* 29, 1415–1424.
- Bunte, K., Swingle, K.W., 2021. Description and development of a database for bedload trap measurements in rocky mountain streams. In: *Gen. Tech. Rep. RMRS-GTR-420. US Department of Agriculture, Forest Service, Rocky Mountain Research Station, Fort Collins, CO*. <https://doi.org/10.2737/RMRS-GTR-420> 420, 24 p.
- Burbank, D.W., Leland, J., Fielding, E., Anderson, R.S., Brozovic, N., Reid, M.R., Duncan, C., 1996. Bedrock incision, rock uplift and threshold hillslopes in the northwestern himalayas. *Nature* 379, 505–510.
- Campforts, B., Shobe, C., Steer, P., Vanmaercke, M., Lague, D., Braun, J., 2020. Hylands 1.0: a hybrid landscape evolution model to simulate the impact of landslides and landslide-derived sediment on landscape evolution. *Geosci. Model Dev.* 13, 3863–3886.
- Carling, P., Tinkler, K., 1998. Conditions for the entrainment of cuboid boulders in bedrock streams: an historical review of literature with respect to recent investigations. *Rivers Over Rock: Fluvial Process Bedrock Channels* 107, 19–34.
- Carling, P.A., Hoffmann, M., Blatter, A.S., 2002. Initial motion of boulders in bedrock channels. *Ancient Floods, Modern Hazards: Principles and Applications of Paleoflood Hydrology* 5, 147–160.
- Carr, J.C., DiBiase, R.A., Erikson, C.M., Kohlman, C.M., 2020. Quantifying changes in bed state and grain mobility in steep bedrock rivers through repeat uav photogrammetry surveys, in: *AGU Fall Meeting 2020*. AGU.
- Carretier, S., Martinod, P., Reich, M., Godderis, Y., 2016. Modelling sediment clasts transport during landscape evolution. *Earth Surface Dynam.* 4, 237–251.
- Carson, M., 1977. Angles of repose, angles of shearing resistance and angles of talus slopes. *Earth Surface Process.* 2, 363–380.
- Chilton, K.D., Spotila, J.A., 2020. Preservation of valley and ridge topography via delivery of resistant, ridge-sourced boulders to hillslopes and channels, southern appalachian mountains, usa. *Geomorphology* 107263.
- Chin, A., Wohl, E., 2005. Toward a theory for step pools in stream channels. *Prog. Phys. Geogr.* 29, 275–296.
- Chin, A., Anderson, S., Collison, A., Ellis-Sugai, B.J., Haltiner, J.P., Hogervorst, J.B., Kondolf, G.M., O'Hirok, L.S., Purcell, A.H., Riley, A.L., et al., 2009. Linking theory and practice for restoration of step-pool streams. *Environ. Manag.* 43, 645–661.
- Church, M., Zimmermann, A., 2007. Form and stability of step-pool channels: Research progress. *Water Resour. Res.* 43.

- Church, M., Stock, R.F., Ryder, J.M., 1979. Contemporary sedimentary environments on baffin island, nwt, canada: debris slope accumulations. *Arct. Alp. Res.* 11, 371–401.
- Church, M., Hassan, M.A., Wolcott, J.F., 1998. Stabilizing self-organized structures in gravel-bed stream channels: Field and experimental observations. *Water Resour. Res.* 34, 3169–3179.
- Clarke, B.A., Burbank, D.W., 2011. Quantifying bedrock-fracture patterns within the shallow subsurface: Implications for rock mass strength, bedrock landslides, and erodibility. *J. Geophys. Res. Earth Surf.* 116.
- Comiti, F., Mao, L., 2012. Recent advances in the dynamics of steep channels. *Gravel-Bed Rivers: Processes, Tools, Environ.* 351–377.
- Comiti, F., Cadol, D., Wohl, E., 2009. Flow regimes, bed morphology, and flow resistance in self-formed step-pool channels. *Water Resour. Res.* 45.
- Cook, K.L., Andermann, C., Gimbert, F., Adhikari, B.R., Hovius, N., 2018. Glacial lake outburst floods as drivers of fluvial erosion in the Himalaya. *Science* 362, 53–57.
- Copons, R., Vilaplana, J., Linares, R., 2009. Rockfall travel distance analysis by using empirical models (sola d'andorra la vella, central pyrenees). *Nat. Hazards Earth Syst. Sci.* 9.
- Cox, R., Jahn, K.L., Watkins, O.G., Cox, P., 2018. Extraordinary boulder transport by storm waves (west of Ireland, winter 2013–2014), and criteria for analysing coastal boulder deposits. *Earth Sci. Rev.* 177, 623–636.
- Croissant, T., Lague, D., Steer, P., Davy, P., 2017. Rapid post-seismic landslide evacuation boosted by dynamic river width. *Nat. Geosci.* 10, 680–684.
- Crouvi, O., Polyakov, V., Pelletier, J., Rasmussen, C., 2015. Decadal-scale soil redistribution along hillslopes in the Mojave Desert. *Earth Surface Dynam.* 3, 251–264.
- Culling, W., 1960. Analytical theory of erosion. *J. Geol.* 68, 336–344.
- Curran, J.C., 2007. Step-pool formation models and associated step spacing. *Earth Surface Process. Landf.* 32, 1611–1627.
- Curran, J.C., Wilcock, P.R., 2005. Characteristic dimensions of the step-pool bed configuration: An experimental study. *Water Resour. Res.* 41.
- Dahal, R.K., Hasegawa, S., Nonomura, A., Yamanaka, M., Masuda, T., Nishino, K., 2008. Gis-based weights-of-evidence modelling of rainfall-induced landslides in small catchments for landslide susceptibility mapping. *Environ. Geol.* 54, 311–324.
- Darmody, R., Thorn, C., Allen, C., 2005. Chemical weathering and boulder mantles, kärkevegge, Swedish Lapland. *Geomorphology* 67, 159–170.
- Davies, T., McSaveney, M., Hodgson, K., 1999. A fragmentation-spreading model for long-runout rock avalanches. *Can. Geotech. J.* 36, 1096–1110.
- Del Vecchio, J., DiBiase, R.A., Denn, A.R., Bierman, P.R., Caffee, M., Zimmerman, S.R., 2018. Record of coupled hillslope and channel response to Pleistocene erosion and deposition in a sandstone headwater valley, central Pennsylvania. *Bulletin* 130, 1903–1917.
- Derriex, F., Siame, L.L., Bourlès, D.L., Chen, R.F., Braucher, R., Léanni, L., Lee, J.C., Chu, H.T., Byrne, T.B., 2014. How fast is the denudation of the Taiwan mountain belt? Perspectives from in situ cosmogenic ¹⁰Be. *J. Asian Earth Sci.* 88, 230–245.
- Deshpande, N., Furbish, D., Arratia, P., Jerolmack, D., 2020. The perpetual fragility of creeping hillslopes. *EarthArXiv*.
- Dethier, D.P., Ouimet, W., Bierman, P.R., Rood, D.H., Balco, G., 2014. Basins and bedrock: Spatial variation in ¹⁰Be erosion rates and increasing relief in the southern Rocky Mountains, USA. *Geology* 42, 167–170.
- DiBiase, R.A., Lamb, M.P., Ganti, V., Booth, A.M., 2017. Slope, grain size, and roughness controls on dry sediment transport and storage on steep hillslopes. *J. Geophys. Res. Earth Surf.* 122, 941–960.
- DiBiase, R.A., Denn, A.R., Bierman, P.R., Kirby, E., West, N., Hidy, A.J., 2018a. Stratigraphic control of landscape response to base-level fall, young woman's creek, Pennsylvania, USA. *Earth Planet. Sci. Lett.* 504, 163–173.
- DiBiase, R.A., Rossi, M.W., Neely, A.B., 2018b. Fracture density and grain size controls on the relief structure of bedrock landscapes. *Geology* 46, 399–402.
- Dietrich, W.E., Bellugi, D.G., Sklar, L.S., Stock, J.D., Heimsath, A.M., Roering, J.J., 2003. Geomorphic transport laws for predicting landscape form and dynamics. *Geophys. Monograph Am. Geophys. Union* 135, 103–132.
- Dini, B., Aaron, J., Manconi, A., De Palezieux, L., Leith, K., Loew, S., 2020. Regional scale investigation of preconditioning factors of rock slope instabilities in NW Bhutan. *J. Geophys. Res. Earth Surf.* 125 (9) e2019JF005404.
- Dini, B., Bennett, G.L., Franco, A.M.A., Whitworth, M.R.Z., Cook, K.L., Senn, A., Reynolds, J.M., 2021. Development of smart boulders to monitor mass movements via the internet of things: a pilot study in Nepal. *Earth Surface Dynam.* 9, 295–315. <https://doi.org/10.5194/esurf-9-295-2021>.
- Doane, T.H., Furbish, D.J., Roering, J.J., Schumer, R., Morgan, D.J., 2018. Nonlocal sediment transport on steep lateral margins, eastern Sierra Nevada, California, USA. *J. Geophys. Res. Earth Surf.* 123, 187–208.
- Dühnforth, M., Anderson, R.S., Ward, D.J., Blum, A., 2012. Unsteady late Pleistocene incision of streams bounding the Colorado front range from measurements of meteoric and in situ ¹⁰Be. *J. Geophys. Res. Earth Surf.* 117.
- Dunning, S., Rosser, N., Petley, D., Massey, C., 2006. Formation and failure of the Tsatichhu landslide dam, Bhutan. *Landslides* 3, 107–113.
- Duszyński, F., Migoń, P., 2015. Boulder aprons indicate long-term gradual and non-catastrophic evolution of cliffed escarpments, Stowowe mts, Poland. *Geomorphology* 250, 63–77.
- Duszyński, F., Jancewicz, K., Kasprzak, M., Migoń, P., 2017. The role of landslides in downslope transport of caprock-derived boulders in sedimentary tablelands, Stowowe mts, SW Poland. *Geomorphology* 295, 84–101.
- Duvall, A., Kirby, E., Burbank, D., 2004. Tectonic and lithologic controls on bedrock channel profiles and processes in coastal California. *J. Geophys. Res. Earth Surf.* 109.
- Eaton, B.C., MacKenzie, L.G., Booker, W.H., 2020. Channel stability in steep gravel-cobble streams is controlled by the coarse tail of the bed material distribution. *Earth Surf. Process. Landf.* 45, 3639–3652.
- Egholm, D.L., Knudsen, M.F., Sandiford, M., 2013. Lifespan of mountain ranges scaled by feedbacks between landsliding and erosion by rivers. *Nature* 498, 475–478.
- Eppes, M.C., Griffing, D., 2010. Granular disintegration of marble in nature: A thermal-mechanical origin for a gully and corestone landscape. *Geomorphology* 117, 170–180.
- Eppes, M.C., Keanini, R., 2017. Mechanical weathering and rock erosion by climate-dependent subcritical cracking. *Rev. Geophys.* 55, 470–508.
- Eppes, M.C., McFadden, L.D., Wegmann, K.W., Scuderi, L.A., 2010. Cracks in desert pavement rocks: Further insights into mechanical weathering by directional insolation. *Geomorphology* 123, 97–108.
- Eppes, M., Magi, B., Scheff, J., Warren, K., Ching, S., Feng, T., 2020. Warmer, wetter climates accelerate mechanical weathering in field data, independent of stress-loading. *Geophys. Res. Lett.* 47 (24) e2020GL089062.
- Erismann, T.H., Abele, G., 2001. Dynamics of Rockslides and Rockfalls. Springer Science & Business Media.
- Fan, X., Dufresne, A., Subramanian, S.S., Strom, A., Hermanns, R., Stefanelli, C.T., Hewitt, K., Yunus, A.P., Dunning, S., Capra, L., et al., 2020. The formation and impact of landslide dams—state of the art. *Earth Sci. Rev.* 203, 103116.
- Ferdowsi, B., Ortiz, C.P., Jerolmack, D.J., 2018. Glassy dynamics of landscape evolution. *Proc. Natl. Acad. Sci.* 115, 4827–4832.
- Ferguson, R., 2007. Flow resistance equations for gravel-and boulder-bed streams. *Water Resour. Res.* 43.
- Ferguson, R., Paola, C., 1997. Bias and precision of percentiles of bulk grain size distributions. *Earth Surface Process Landf.* 22, 1061–1077.
- Fernandez Luque, R., Van Beek, R., 1976. Erosion and transport of bed-load sediment. *J. Hydraul. Res.* 14, 127–144.
- Finnegan, N.J., Broudy, K.N., Nereson, A.L., Roering, J.J., Handwerker, A.L., Bennett, G., 2019. River channel width controls blocking by slow-moving landslides in California's Franciscan mélange. *Earth Surface Dynam.* 7, 6879–6894.
- Fletcher, R.C., Brantley, S.L., 2010. Reduction of bedrock blocks as corestones in the weathering profile: observations and model. *Am. J. Sci.* 310, 131–164.
- Foufoula-Georgiou, E., Ganti, V., Dietrich, W., 2010. A nonlocal theory of sediment transport on hillslopes. *J. Geophys. Res. Earth Surf.* 115.
- Fritz, S.J., Mohr, D.W., 1984. Chemical alteration in the micro weathering environment within a spheroidally-weathered anorthosite boulder. *Geochim. Cosmochim. Acta* 48, 2527–2535.
- Fuller, T.K., Gran, K.B., Sklar, L.S., Paola, C., 2016. Lateral erosion in an experimental bedrock channel: The influence of bed roughness on erosion by bed load impacts. *J. Geophys. Res. Earth Surf.* 121, 1084–1105.
- Furbish, D.J., Roering, J.J., 2013. Sediment disentrainment and the concept of local versus nonlocal transport on hillslopes. *J. Geophys. Res. Earth Surf.* 118, 937–952.
- Furbish, D.J., Roering, J.J., Doane, T.H., Roth, D.L., Williams, S.G., Abbott, A.M., 2020a. Rarefied particle motions on hillslopes: 1. theory. *Earth Surface Dyn. Discuss.* 1–63.
- Furbish, D.J., Williams, S.G.W., Roth, D.L., Doane, T.H., Roering, J.J., 2020b. Rarefied particle motions on hillslopes: 2. analysis. *Earth Surface Dyn. Discuss.* 1–58. URL: <https://esurf.copernicus.org/preprints/esurf-2020-99/>. <https://doi.org/10.5194/esurf-2020-99>.
- Gabet, E.J., 2003. Sediment transport by dry ravel. *J. Geophys. Res. Solid Earth* 108.
- Gabet, E.J., Mendoza, M.K., 2012. Particle transport over rough hillslope surfaces by dry ravel: Experiments and simulations with implications for nonlocal sediment flux. *J. Geophys. Res. Earth Surf.* 117.
- Gallen, S.F., Wegmann, K.W., Frankel, K.L., Hughes, S., Lewis, R.Q., Lyons, N., Paris, P., Ross, K., Bauer, J.B., Witt, A.C., 2011. Hillslope response to knickpoint migration in the southern Appalachians: implications for the evolution of post-orogenic landscapes. *Earth Surf. Process. Landf.* 36, 1254–1267.
- Gilbert, G.K., 1877. Geology of the Henry mountains. In: Technical Report. Government Printing Office.
- Gilbert, G.K., 1909. The convexity of hilltops. *J. Geol.* 17, 344–350.
- Gioia, G., Bombardelli, F., 2001. Scaling and similarity in rough channel flows. *Phys. Rev. Lett.* 88, 014501.
- Glade, R., Anderson, R., 2018. Quasi-steady evolution of hillslopes in layered landscapes: An analytic approach. *J. Geophys. Res. Earth Surf.* 123, 26–45.
- Glade, R.C., Anderson, R.S., Tucker, G.E., 2017. Block-controlled hillslope form and persistence of topography in rocky landscapes. *Geology* 45, 311–314.
- Glade, R.C., Shobe, C.M., Anderson, R.S., Tucker, G.E., 2019. Canyon shape and erosion dynamics governed by channel-hillslope feedbacks. *Geology* 47, 650–654.
- Godard, V., Bourlès, D.L., Spinabella, F., Burbank, D.W., Bookhagen, B., Fisher, G.B., Moulin, A., Léanni, L., 2014. Dominance of tectonics over climate in Himalayan denudation. *Geology* 42, 243–246.
- Golly, A., Turowski, J.M., Badoux, A., Hovius, N., 2017. Controls and feedbacks in the coupling of mountain channels and hillslopes. *Geology* 45, 307–310.
- Golly, A., Turowski, J.M., Badoux, A., Hovius, N., 2019. Testing models of step formation against observations of channel steps in a steep mountain stream. *Earth Surf. Process. Landf.* 44, 1390–1406.
- Gould, S.J., 1985. The median isn't the message. *Discover* 6, 40–42.
- Granger, D.E., Kirchner, J.W., Finkel, R.C., 1997. Quaternary downcutting rate of the new river, Virginia, measured from differential decay of cosmogenic ²⁶Al and ¹⁰Be in cave-deposited alluvium. *Geology* 25, 107–110.
- Granger, D.E., Riebe, C.S., Kirchner, J.W., Finkel, R.C., 2001. Modulation of erosion on steep granitic slopes by boulder armoring, as revealed by cosmogenic ²⁶Al and ¹⁰Be. *Earth Planet. Sci. Lett.* 186, 269–281.
- Grant, G.E., Swanson, F.J., Wolman, M.G., 1990. Pattern and origin of stepped-bed morphology in high-gradient streams, western Cascades, Oregon. *Geol. Soc. Am. Bull.* 102, 340–352.
- Greenbaum, N., Schwartz, U., Carling, P., Bergman, N., Mushkin, A., Zituni, R., Halevi, R., Benito, G., Porat, N., 2020. Frequency of boulders transport during large

- floods in hyperarid areas using paleoflood analysis—an example from the negev desert, israel. *Earth Sci. Rev.* 202, 103086.
- Guzzetti, F., Reichenbach, P., Cardinali, M., Galli, M., Ardizzone, F., 2005. Probabilistic landslide hazard assessment at the basin scale. *Geomorphology* 72, 272–299.
- Hack, J.T., 1965. Geomorphology of the Shenandoah Valley, Virginia, and West Virginia, and Origin of the Residual Ore Deposits. US Government Printing Office.
- Hales, T., Roering, J.J., 2007. Climatic controls on frost cracking and implications for the evolution of bedrock landscapes. *J. Geophys. Res. Earth Surf.* 112.
- Hancock, G.S., Anderson, R.S., Whipple, K.X., 1998. Beyond power: Bedrock river incision process and form. *Geophys. Monograph Am. Geophys. Union* 107, 35–60.
- Harvey, A., 2001. Coupling between hillslopes and channels in upland fluvial systems: implications for landscape sensitivity, illustrated from the howgill fells, northwest england. *Catena* 42, 225–250.
- Hasbargen, L.E., Paola, C., 2000. Landscape instability in an experimental drainage basin. *Geology* 28, 1067–1070.
- Hendrick, R.R., Ely, L.L., Papanicolaou, A., 2010. The role of hydrologic processes and geomorphology on the morphology and evolution of sediment clusters in gravel-bed rivers. *Geomorphology* 114, 483–496.
- Hey, R.D., 1979. Flow resistance in gravel-bed rivers. *J. Hydraul. Div.* 105, 365–379.
- Houssais, M., Jerolmack, D.J., 2017. Toward a unifying constitutive relation for sediment transport across environments. *Geomorphology* 277, 251–264.
- Howard, A.D., 1994. A detachment-limited model of drainage basin evolution. *Water Resour. Res.* 30, 2261–2285.
- Howard, A.D., 1998. Long profile development of bedrock channels: Interaction of weathering, mass wasting, bed erosion, and sediment transport. *Geophys. Monograph Am. Geophys. Union* 107, 297–319.
- Howard, A., Dolan, R., 1981. Geomorphology of the colorado river in the grand canyon. *J. Geol.* 89, 269–298.
- Howard, A.D., Kochel, R., 1988. Introduction to cuesta landforms and sapping processes on the colorado plateau. *Sapping Features of the Colorado Plateau: A Comparative Planetary Geology Field Guide* 491, 6–56.
- Howard, A., Selby, M., 1994. *Rock Slopes*, Edited by Ad Abrahams and Aj Parsons.
- Huber, M.L., Lupker, M., Gallen, S.F., Christl, M., Gajurel, A.P., 2020. Timing of exotic, far-traveled boulder emplacement and paleo-outburst flooding in the central himalayas. *Earth Surface Dynam.* 8, 769–787.
- Hungr, O., Corominas, J., Eberhardt, E., et al., 2005. Estimating landslide motion mechanism, travel distance and velocity. *Landslide Risk Manag.* 1, 99–128.
- Hurst, M.D., Mudd, S.M., Walcott, R., Attal, M., Yoo, K., 2012. Using hilltop curvature to derive the spatial distribution of erosion rates. *J. Geophys. Res. Earth Surf.* 117.
- Jaeger, J.C., Carslaw, H.S., 1959. *Conduction of Heat in Solids*. Clarendon P.
- Johnson, J.P., Whipple, K.X., Sklar, L.S., Hanks, T.C., 2009. Transport slopes, sediment cover, and bedrock channel incision in the henry mountains, utah. *J. Geophys. Res. Earth Surf.* 114.
- Judd, H.E., Peterson, D.F., 1969. *Hydraulics of large bed element channels*. Utah Water Research Laboratory Report.
- Kalathil, S.T., Chandra, V., 2019. Review of step-pool hydrodynamics in mountain streams. *Progr. Phys. Geogr. Earth Environ.* 43, 607–626.
- Kargel, J.S., Leonard, G.J., Shugar, D.H., Haritashya, U.K., Bevington, A., Fielding, E., Fujita, K., Geertsema, M., Miles, E., Steiner, J., et al., 2016. Geomorphic and geologic controls of geohazards induced by nepal's 2015 gorkha earthquake. *Science* 351.
- Katul, G., Wiberg, P., Albertson, J., Hornberger, G., 2002. A mixing layer theory for flow resistance in shallow streams. *Water Resour. Res.* 38, 1–32.
- Kean, J.W., Smith, J.D., 2006a. Form drag in rivers due to small-scale natural topographic features: 1. regular sequences. *J. Geophys. Res. Earth Surf.* 111.
- Kean, J.W., Smith, J.D., 2006b. Form drag in rivers due to small-scale natural topographic features: 2. irregular sequences. *J. Geophys. Res. Earth Surf.* 111.
- Kean, J.W., Smith, J.D., 2010. Calculation of stage-discharge relations for gravel bedded channels. *J. Geophys. Res. Earth Surf.* 115.
- Kean, J.W., Staley, D.M., Lancaster, J.T., Rengers, F.K., Swanson, B.J., Coe, J.A., Hernandez, J., Sigman, A., Allstadt, K.E., Lindsay, D.N., 2019. Inundation, flow dynamics, and damage in the 9 january 2018 montecito debris-flow event, california, usa: Opportunities and challenges for post-wildfire risk assessment. *Geosphere* 15, 1140–1163.
- Keulegan, G.H., 1938. *Laws of turbulent flow in open channels*, volume 21. National Bureau of Standards US.
- King, L.C., 1953. Canons of landscape evolution. *Geol. Soc. Am. Bull.* 64, 721–752.
- King, C., 1957. The uniformitarian nature of hillslopes. *Transact. Edinburgh Geological Society* 17, 81–102.
- Kirkby, M., Statham, I., 1975. Surface stone movement and scree formation. *J. Geol.* 83, 349–362.
- Kolmogorov, A.N., 1941. The local structure of turbulence in incompressible viscous fluid for very large reynolds numbers. *Cr Acad. Sci. URSS* 30, 301–305.
- Koons, E.D., 1955. Cliff retreat in the southwestern united states. *Am. J. Sci.* 253, 44–52.
- Korup, O., 2006. Rock-slope failure and the river long profile. *Geology* 34, 45–48.
- Korup, O., Strom, A.L., Weidinger, J.T., 2006. Fluvial response to large rock-slope failures: Examples from the himalayas, the tien shan, and the southern alps in new zealand. *Geomorphology* 78, 3–21.
- Korup, O., Densmore, A.L., Schlunegger, F., 2010. The role of landslides in mountain range evolution. *Geomorphology* 120, 77–90.
- Kritikos, T., Robinson, T.R., Davies, T.R., 2015. Regional coseismic landslide hazard assessment without historical landslide inventories: A new approach. *J. Geophys. Res. Earth Surf.* 120, 711–729.
- Lague, D., 2014. The stream power river incision model: evidence, theory and beyond. *Earth Surf. Process. Landf.* 39, 38–61.
- Lamb, M.P., Dietrich, W.E., Venditti, J.G., 2008. Is the critical shields stress for incipient sediment motion dependent on channel-bed slope? *J. Geophys. Res. Earth Surf.* 113.
- Lamb, M.P., Finnegan, N.J., Scheingross, J.S., Sklar, L.S., 2015. New insights into the mechanics of fluvial bedrock erosion through flume experiments and theory. *Geomorphology* 244, 33–55.
- Lamp, J., Marchant, D., Mackay, S., Head, J., 2017. Thermal stress weathering and the spalling of antarctic rocks. *J. Geophys. Res. Earth Surf.* 122, 3–24.
- Laronne, J., Carson, M., 1976. Interrelationships between bed morphology and bed-material transport for a small, gravel-bed channel. *Sedimentology* 23, 67–85.
- Larsen, I.J., Montgomery, D.R., 2012. Landslide erosion coupled to tectonics and river incision. *Nat. Geosci.* 5, 468–473.
- Lavé, J., Avouac, J.P., 2001. Fluvial incision and tectonic uplift across the himalayas of central nepal. *J. Geophys. Res. Solid Earth* 106, 26561–26591.
- Lawrence, D., 1997. Macroscale surface roughness and frictional resistance in overland flow. *Earth Surface Process Landf.* 22, 365–382.
- Le Bouteiller, C., Naaim-Bouvet, F., Mathys, N., Lavé, J., 2011. A new framework for modeling sediment fining during transport with fragmentation and abrasion. *J. Geophys. Res. Earth Surf.* 116.
- Lenzi, M.A., 2001. Step-pool evolution in the rio cordon, northeastern italy. *Earth Surf. Process. Landf.* 26, 991–1008.
- Lenzi, M.A., 2002. Stream bed stabilization using boulder check dams that mimic step-pool morphology features in northern italy. *Geomorphology* 45, 243–260.
- Lenzi, M.A., 2004. Displacement and transport of marked pebbles, cobbles and boulders during floods in a steep mountain stream. *Hydrol. Process.* 18, 1899–1914.
- Leopold, L., 1992. Sediment size that determines channel morphology. *Dynam. Gravel-Bed Rivers* 297–311.
- Li, G., West, A.J., Densmore, A.L., Hammond, D.E., Jin, Z., Zhang, F., Wang, J., Hilton, R. G., 2016. Connectivity of earthquake-triggered landslides with the fluvial network: Implications for landslide sediment transport after the 2008 wenchuan earthquake. *J. Geophys. Res. Earth Surf.* 121, 703–724.
- Li, T., Fuller, T.K., Sklar, L.S., Gran, K.B., Venditti, J.G., 2020. A mechanistic model for lateral erosion of bedrock channel banks by bedload particle impacts. *J. Geophys. Res. Earth Surf.* 125, e2019JF005509.
- Linton, D.L., 1955. The problem of tors. *Geogr. J.* 121, 470–487.
- Locat, P., Couture, R., Leroueil, S., Locat, J., Jaboyedoff, M., 2006. Fragmentation energy in rock avalanches. *Can. Geotech. J.* 43, 830–851.
- MacKenzie, L.G., Eaton, B.C., 2017. Large grains matter: contrasting bed stability and morphodynamics during two nearly identical experiments. *Earth Surf. Process. Landf.* 42, 1287–1295.
- MacKenzie, L.G., Eaton, B.C., Church, M., 2018. Breaking from the average: Why large grains matter in gravel-bed streams. *Earth Surf. Process. Landf.* 43, 3190–3196.
- Malamud, B.D., Turcotte, D.L., Guzzetti, F., Reichenbach, P., 2004. Landslide inventories and their statistical properties. *Earth Surf. Process. Landf.* 29, 687–711.
- Marc, O., Turowski, J.M., Meunier, P., 2021. Controls on the grain size distribution of landslides in Taiwan: the influence of drop height, scar depth and bedrock strength. *Earth Surface Dyn. Discuss.* 2021, 1–23. <https://doi.org/10.5194/esurf-2021-19>.
- Marchetti, D.W., Hynes, S.A., Cerling, T.E., 2012. Gravel-capped benches above northern tributaries of the escalante river, south-central utah. *Geosphere* 8, 835–853.
- Marshall, J.A., Sklar, L.S., 2012. Mining soil databases for landscape-scale patterns in the abundance and size distribution of hillslope rock fragments. *Earth Surf. Process. Landf.* 37, 287–300.
- Marcotte, A.L., Neudorf, C.M., Langston, A.L., 2021. Lateral bedrock erosion and valley formation in a heterogeneously layered landscape, Northeast Kansas. *Earth Surface Processes and Landforms*. <https://doi.org/10.1002/esp.5172>.
- Marshall, J., Roering, J., Rempel, A., Shafer, S., Bartlein, P., 2021. Extensive frost weathering across unglaciated north america during the last glacial maximum. *Geophys. Res. Lett.* 48, e2020GL090305.
- Martin, Y., Church, M., 1997. Diffusion in landscape development models: on the nature of basic transport relations. *Earth Surface Process. Landf.* 22, 273–279.
- McGrath, G.S., Nie, Z., Dyskin, A., Byrd, T., Jenner, R., Holbeche, G., Hinz, C., 2013. In situ fragmentation and rock particle sorting on arid hills. *J. Geophys. Res. Earth Surf.* 118, 17–28.
- Menting, F., Langston, A.L., Temme, A.J., 2015. Downstream fining, selective transport, and hillslope influence on channel bed sediment in mountain streams, colorado front range, usa. *Geomorphology* 239, 91–105.
- Messenzehl, K., Viles, H., Otto, J.C., Ewald, A., Dikau, R., 2018. Linking rock weathering, rockwall instability and rockfall supply on talus slopes in glaciated hanging valleys (swiss alps). *Permafrost. Periglac. Process.* 29, 135–151.
- Meyer-Peter, E., Müller, R., 1948. Formulas for bed-load transport, in: IAHSR 2nd meeting, Stockholm, appendix 2. IAHR.
- Michaelides, K., Martin, G.J., 2012. Sediment transport by runoff on debris-mantled dryland hillslopes. *J. Geophys. Res. Earth Surf.* 117.
- Mills, H.H., 1981. Boulder deposits and the retreat of mountain slopes, or, "gully gravure" revisited. *J. Geol.* 89, 649–660.
- Mills, H.H., 1989. Hollow form as a function of boulder size in the valley and ridge province, southwestern virginia. *Geology* 17, 595–598.
- Molnar, P., Anderson, R.S., Anderson, S.P., 2007. Tectonics, fracturing of rock, and erosion. *J. Geophys. Res. Earth Surf.* 112.
- Molnar, P., Densmore, A.L., Mcardell, B.W., Turowski, J.M., Burlando, P., 2010. Analysis of changes in the step-pool morphology and channel profile of a steep mountain stream following a large flood. *Geomorphology* 124, 85–94.
- Monsalve, A., Yager, E., 2017. Bed surface adjustments to spatially variable flow in low relative submergence regimes. *Water Resour. Res.* 53, 9350–9367.
- Montgomery, D.R., Buffington, J.M., 1997. Channel-reach morphology in mountain drainage basins. *Geol. Soc. Am. Bull.* 109, 596–611.
- Moon, B., 1984. The forms of rock slopes in the cape fold mountains. *S. Afr. Geogr. J.* 66, 16–31.

- Morche, D., Schmidt, K.H., 2012. Sediment transport in an alpine river before and after a dambreak flood event. *Earth Surf. Process. Landf.* 37, 347–353.
- Murphy, B.P., Johnson, J.P., Gasparini, N.M., Hancock, G.S., Small, E.E., 2018. Weathering and abrasion of bedrock stambed topography. *Geology* 46, 459–462.
- Nativ, R., Turowski, J.M., Goren, L., Laronne, J., Hovius, N., 2019. Theoretical prediction and field examination of bedrock channel morphology in boulder-dominated fluvial reaches along the liwu catchment, taiwan. *Geophys. Res. Abstr.* 21.
- Neely, A.B., DiBiase, R.A., 2020. Drainage area, bedrock fracture spacing, and weathering controls on landscape-scale patterns in surface sediment grain size. *J. Geophys. Res. Earth Surf.* 125 (10) e2020JF005560.
- Neely, A.B., DiBiase, R.A., Corbett, L.B., Bierman, P.R., Caffee, M.W., 2019. Bedrock fracture density controls on hillslope erodibility in steep, rocky landscapes with patchy soil cover, southern california, usa. *Earth Planet. Sci. Lett.* 522, 186–197.
- Nitsche, M., Rickenmann, D., Turowski, J.M., Badoux, A., Kirchner, J.W., 2011. Evaluation of bedload transport predictions using flow resistance equations to account for macro-roughness in steep mountain streams. *Water Resour. Res.* 47.
- Nitsche, M., Rickenmann, D., Kirchner, J.W., Turowski, J., Badoux, A., 2012. Macroroughness and variations in reach-averaged flow resistance in steep mountain streams. *Water Resour. Res.* 48.
- Ott, R.F., 2020. How lithology impacts global topography, vegetation, and animal biodiversity: A global-scale analysis of mountainous regions. *Geophys. Res. Lett.* 47 e2020GL088649.
- Quimet, W.B., Whipple, K.X., Royden, L.H., Sun, Z., Chen, Z., 2007. The influence of large landslides on river incision in a transient landscape: Eastern margin of the tibetan plateau (sichuan, china). *Geol. Soc. Am. Bull.* 119, 1462–1476.
- Quimet, W., Whipple, K., Crosby, B., Johnson, J., Schildgen, T., 2008. Epigenetic gorges in fluvial landscapes. *Earth Surface Process. Landf.* 33, 1993–2009.
- Pagliara, S., Chiavaccini, P., 2006. Flow resistance of rock chutes with protruding boulders. *J. Hydraul. Eng.* 132, 545–552.
- Palucis, M., Lamb, M., 2017. What controls channel form in steep mountain streams? *Geophys. Res. Lett.* 44, 7245–7255.
- Papanicolaou, A., Tsakiris, A.G., Wyssmann, M.A., Kramer, C.M., 2018. Boulder array effects on bedload pulses and depositional patches. *J. Geophys. Res. Earth Surf.* 123, 2925–2953.
- Parker, R., Hancox, G., Petley, D., Massey, C., Densmore, A., Rosser, N., 2015. Spatial distributions of earthquake-induced landslides and hillslope preconditioning in northwest south island, new zealand. *Earth Surface Dynamics*, 3, 501–525.
- Perras, M.A., Diederichs, M.S., 2014. A review of the tensile strength of rock: concepts and testing. *Geotech. Geol. Eng.* 32, 525–546.
- Pfeiffer, A.M., Finnegan, N.J., 2018. Regional variation in gravel riverbed mobility, controlled by hydrologic regime and sediment supply. *Geophys. Res. Lett.* 45, 3097–3106.
- Phillips, C.B., Jerolmack, D.J., 2016. Self-organization of river channels as a critical filter on climate signals. *Science* 352, 694–697.
- Poesen, J., Torri, D., Bunte, K., 1994. Effects of rock fragments on soil erosion by water at different spatial scales: a review. *Catena* 23, 141–166.
- Polvi, L.E., 2021. Morphodynamics of boulder-bed semi-alluvial streams in northern fennoscandia: a flume experiment to determine sediment self-organization. *Water Resour. Res.* 57 e2020WR028859.
- Prancevic, J.P., Lamb, M.P., 2015. Unraveling bed slope from relative roughness in initial sediment motion. *J. Geophys. Res. Earth Surf.* 120, 474–489.
- Prancevic, J., Sklar, L.S., Dietrich, W.E., 2020. Modeling how rivers digest boulders: long residence times and coarse riverbed surfaces lead to preferential wear of boulders through in-place abrasion, in: AGU Fall Meeting 2020. AGU.
- Prandtl, L., 1925. 7. bericht über untersuchungen zur ausgebildeten turbulenz. *ZAMM-Journal of Applied Mathematics and Mechanics/Zeitschrift für Angewandte Mathematik und Mechanik* 5, 136–139.
- Putkonen, J., Morgan, D., Balco, G., 2014. Boulder weathering in mcmurdo dry valleys, antarctica. *Geomorphology* 219, 192–199.
- Raming, L.W., Whipple, K.X., 2020. Canyon formation on the hawaiian islands: Can a single threshold of river incision explain observed patterns of incision? In: *Geological Society of America Abstracts with Programs*, p. 52. <https://doi.org/10.1130/abs/2020AM-359366>.
- Regmi, A.D., Dhital, M.R., Zhang, J.q., Su, L.j., Chen, X.q., 2016. Landslide susceptibility assessment of the region affected by the 25 april 2015 gorkha earthquake of nepal. *J. Mt. Sci.* 13, 1941–1957.
- Rengers, F.K., Kean, J.W., Reitman, N.G., Smith, J.B., Coe, J.A., McGuire, L.A., 2020. The influence of frost weathering on debris flow sediment supply in an alpine basin. *Journal of Geophysical Research: Earth Surface* 125, e2019JF005369.
- Rickenmann, D., 2001. Comparison of bed load transport in torrents and gravel bed streams. *Water Resour. Res.* 37, 3295–3305.
- Rickenmann, D., Recking, A., 2011. Evaluation of flow resistance in gravel-bed rivers through a large field data set. *Water Resour. Res.* 47.
- Rickenmann, D., Chiari, M., Friedl, K., 2006. Setrac—a sediment routing model for steep torrent channels. In: *River Flow*. Taylor & Francis London, pp. 843–852.
- Riebe, C.S., Sklar, L.S., Lukens, C.E., Shuster, D.L., 2015. Climate and topography control the size and flux of sediment produced on steep mountain slopes. *Proceedings of the National Academy of Sciences*. <https://doi.org/10.1073/pnas.1503567112>.
- Roda-Boluda, D.C., D'Arcy, M., McDonald, J., Whittaker, A.C., 2018. Lithological controls on hillslope sediment supply: insights from landslide activity and grain size distributions. *Earth Surf. Process. Landf.* 43, 956–977.
- Rodine, J.D., Johnson, A.M., 1976. The ability of debris, heavily freighted with coarse clastic materials, to flow on gentle slopes. *Sedimentology* 23, 213–234.
- Roering, J.J., Kirchner, J.W., Dietrich, W.E., 1999. Evidence for nonlinear, diffusive sediment transport on hillslopes and implications for landscape morphology. *Water Resour. Res.* 35, 853–870.
- Roering, J.J., Kirchner, J.W., Dietrich, W.E., 2001a. Hillslope evolution by nonlinear, slope-dependent transport: Steady state morphology and equilibrium adjustment timescales. *J. Geophys. Res. Solid Earth* 106, 16499–16513.
- Roering, J.J., Kirchner, J.W., Sklar, L.S., Dietrich, W.E., 2001b. Hillslope evolution by nonlinear creep and landsliding: An experimental study. *Geology* 29, 143–146.
- Roering, J.J., Perron, J.T., Kirchner, J.W., 2007. Functional relationships between denudation and hillslope form and relief. *Earth Planet. Sci. Lett.* 264, 245–258.
- Roering, J.J., Mackey, B.H., Handwerker, A.L., Booth, A.M., Schmidt, D.A., Bennett, G.L., Cerovski-Darriau, C., 2015. Beyond the angle of repose: A review and synthesis of landslide processes in response to rapid uplift, eel river, northern california. *Geomorphology* 236, 109–131.
- Roth, D.L., Doane, T.H., Roering, J.J., Furbish, D.J., Zettler-Mann, A., 2020. Particle motion on burned and vegetated hillslopes. *Proc. Natl. Acad. Sci.* 117 (41), 25335–25343.
- Ruiz-Carulla, R., Corominas, J., 2020. Analysis of rockfalls by means of a fractal fragmentation model. *Rock Mech. Rock. Eng.* 53, 1433–1455.
- Ruiz-Carulla, R., Corominas, J., Mavrouli, O., 2015. A methodology to obtain the block size distribution of fragmental rockfall deposits. *Landslides* 12, 815–825.
- Ruiz-Carulla, R., Corominas, J., Mavrouli, O., 2017. A fractal fragmentation model for rockfalls. *Landslides* 14, 875–889.
- Saletti, M., Hassan, M.A., 2020. Width variations control the development of grain structuring in steep step-pool dominated streams: insight from flume experiments. *Earth Surf. Process. Landf.* 45, 1430–1440.
- Schanz, S.A., Montgomery, D.R., 2016. Lithologic controls on valley width and strath terrace formation. *Geomorphology* 258, 58–68.
- Scheingross, J.S., Minchew, B.M., Mackey, B.H., Simons, M., Lamb, M.P., Hensley, S., 2013. Fault-zone controls on the spatial distribution of slow-moving landslides. *Bulletin* 125, 473–489.
- Scherler, D., DiBiase, R.A., Fisher, G.B., Avouac, J.P., 2017. Testing monsoonal controls on bedrock river incision in the himalaya and eastern tibet with a stochastic-threshold stream power model. *J. Geophys. Res. Earth Surf.* 122, 1389–1429.
- Schildgen, T., Dethier, D.P., Bierman, P., Caffee, M., 2002. 26al and 10be dating of late pleistocene and holocene fill terraces: a record of fluvial deposition and incision, colorado front range. *Earth Surface Process. Landf.* 27, 773–787.
- Schlömer, O., Grams, P.E., Buscombe, D., Herget, J., 2021. Geometry of obstacle marks at instream boulders – integration of laboratory investigations and field observations. *Earth Surface Process. Landf.* <https://doi.org/10.1002/esp.5055>.
- Schneider, J.M., Rickenmann, D., Turowski, J.M., Bunte, K., Kirchner, J.W., 2015. Applicability of bed load transport models for mixed-size sediments in steep streams considering macro-roughness. *Water Resour. Res.* 51, 5260–5283.
- Schumm, S., Stevens, M., 1973. Abrasion in place: a mechanism for rounding and size reduction of coarse sediments in rivers. *Geology* 1, 37–40.
- Scott, D.N., Wohl, E.E., 2019. Bedrock fracture influences on geomorphic process and form across process domains and scales. *Earth Surf. Process. Landf.* 44, 27–45.
- Seidl, M.A., Dietrich, W.E., Kirchner, J.W., 1994. Longitudinal profile development into bedrock: An analysis of hawaiian channels. *J. Geol.* 102, 457–474.
- Selby, M.J., 1987. Rock slopes. *Slope Stab.* 475–504.
- Shobe, C.M., Tucker, G.E., Anderson, R.S., 2016. Hillslope-derived blocks retard river incision. *Geophys. Res. Lett.* 43, 5070–5078.
- Shobe, C.M., Tucker, G.E., Rossi, M.W., 2018. Variable-threshold behavior in rivers arising from hillslope-derived blocks. *J. Geophys. Res. Earth Surf.* 123, 1931–1957.
- Shobe, C.M., Bennett, G.L., Tucker, G.E., Roback, K., Miller, S.R., Roering, J.J., 2020. Boulders as a lithologic control on river and landscape response to tectonic forcing at the mendocino triple junction. *Geol. Soc. Am. Bull.* 133, 647–662.
- Shobe, C.M., Turowski, J.M., Nativ, R., Glade, R.C., Bennett, G.L., Dini, B., 2021. Data to accompany “The role of infrequently mobile boulders in modulating landscape evolution and geomorphic hazards” <https://doi.org/10.6084/m9.figshare.14725503>.
- Sklar, L., Dietrich, W.E., 1998. River longitudinal profiles and bedrock incision models: Stream power and the influence of sediment supply. *Geophys. Monograph Am. Geophys. Union* 107, 237–260.
- Sklar, L.S., Dietrich, W.E., 2004. A mechanistic model for river incision into bedrock by saltating bed load. *Water Resour. Res.* 40.
- Sklar, L.S., Riebe, C.S., Marshall, J.A., Genetti, J., Leclere, S., Lukens, C.L., Mercus, V., 2017. The problem of predicting the size distribution of sediment supplied by hillslopes to rivers. *Geomorphology* 277, 31–49.
- Sklar, L.S., Riebe, C.S., Genetti, J., Leclere, S., Lukens, C.E., 2020. Downvalley fining of hillslope sediment in an alpine catchment: implications for downstream fining of sediment flux in mountain rivers. *Earth Surf. Process. Landf.* 45, 1828–1845.
- Spencer, D.W., 1963. The interpretation of grain size distribution curves of clastic sediments. *J. Sediment. Res.* 33, 180–190.
- Spreafico, M.C., Cervi, F., Francioni, M., Stead, D., Borgatti, L., 2017. An investigation into the development of toppling at the edge of fractured rock plateaux using a numerical modelling approach. *Geomorphology* 288, 83–98.
- Stanley, T., Kirschbaum, D.B., 2017. A heuristic approach to global landslide susceptibility mapping. *Nat. Hazards* 87, 145–164.
- Statham, I., 1976. A scree slope rockfall model. *Earth Surface Process.* 1, 43–62.
- Terry, J., Goff, J., 2014. Megaclasts: Proposed revised nomenclature at the coarse end of the udden-wentworth grain-size scale for sedimentary particles revised nomenclature at the coarse end of the udden-wentworth scale. *J. Sediment. Res.* 84, 192–197.
- Thaler, E., Covington, M.D., 2016. The influence of sandstone caprock material on bedrock channel steepness within a tectonically passive setting: Buffalo national river basin, arkansas, usa. *J. Geophys. Res. Earth Surf.* 121, 1635–1650.
- Tofelde, S., Duesing, W., Schildgen, T.F., Wickert, A.D., Wittmann, H., Alonso, R.N., Strecker, M., 2018. Effects of deep-seated versus shallow hillslope processes on

- cosmogenic ¹⁰Be concentrations in fluvial sand and gravel. *Earth Surf. Process. Landf.* 43, 3086–3098.
- Tucker, G.E., Bradley, D.N., 2010. Trouble with diffusion: Reassessing hillslope erosion laws with a particle-based model. *J. Geophys. Res. Earth Surf.* 115.
- Turowski, J.M., Lague, D., Hovius, N., 2007. Cover effect in bedrock abrasion: A new derivation and its implications for the modeling of bedrock channel morphology. *J. Geophys. Res. Earth Surf.* 112.
- Turowski, J.M., Lague, D., Hovius, N., 2009a. Response of bedrock channel width to tectonic forcing: Insights from a numerical model, theoretical considerations, and comparison with field data. *J. Geophys. Res. Earth Surf.* 114.
- Turowski, J.M., Yager, E.M., Badoux, A., Rickenmann, D., Molnar, P., 2009b. The impact of exceptional events on erosion, bedload transport and channel stability in a step-pool channel. *Earth Surf. Process. Landf.* 34, 1661–1673.
- Turzewski, M.D., Huntington, K.W., LeVeque, R.J., 2019. The geomorphic impact of outburst floods: Integrating observations and numerical simulations of the 2000 Yigong flood, eastern Himalaya. *J. Geophys. Res. Earth Surf.* 124, 1056–1079.
- Udden, J.A., 1914. Mechanical composition of clastic sediments. *Geol. Soc. Am. Bull.* 25, 655–744.
- Vanoni, V., 1975. Sediment discharge formulas. *Sediment. Eng.* 190–229.
- Verdian, J.P., Sklar, L.S., Riebe, C.S., Moore, J.R., 2020. Sediment size on talus slopes correlates with fracture spacing on bedrock cliffs: Implications for predicting initial sediment size distributions on hillslopes. *Earth Surface Dyn. Discuss.* 2020, 1–23. <https://doi.org/10.5194/esurf-2020-54>.
- Wahrhaftig, C., 1965. Stepped topography of the southern Sierra Nevada, California. *Geol. Soc. Am. Bull.* 76, 1165–1190.
- Ward, D.J., 2019. Dip, layer spacing, and incision rate controls on the formation of strike valleys, cuestas, and cliffbands in heterogeneous stratigraphy. *Lithosphere* 11, 697–707.
- Ward, D.J., Spotila, J.A., Hancock, G.S., Galbraith, J.M., 2005. New constraints on the late Cenozoic incision history of the New River, Virginia. *Geomorphology* 72, 54–72.
- Ward, D., Berlin, M., Anderson, R., 2011. Sediment dynamics below retreating cliffs. *Earth Surf. Process. Landf.* 36, 1023–1043.
- Wentworth, C.K., 1922. A scale of grade and class terms for clastic sediments. *J. Geol.* 30, 377–392.
- Whipple, K.X., 2001. Fluvial landscape response time: how plausible is steady-state denudation? *Am. J. Sci.* 301, 313–325.
- Whipple, K.X., 2004. Bedrock rivers and the geomorphology of active orogens. *Annu. Rev. Earth Planet. Sci.* 32, 151–185.
- Whipple, K.X., Dunne, T., 1992. The influence of debris-flow rheology on fan morphology, Owens Valley, California. *Geol. Soc. Am. Bull.* 104, 887–900.
- Whipple, K.X., Tucker, G.E., 1999. Dynamics of the stream-power river incision model: Implications for height limits of mountain ranges, landscape response timescales, and research needs. *J. Geophys. Res. Solid Earth* 104, 17661–17674.
- Whipple, K.X., Hancock, G.S., Anderson, R.S., 2000. River incision into bedrock: Mechanics and relative efficacy of plucking, abrasion, and cavitation. *Geol. Soc. Am. Bull.* 112, 490–503.
- Whitbread, K., Jansen, J., Bishop, P., Attal, M., 2015. Substrate, sediment, and slope controls on bedrock channel geometry in postglacial streams. *J. Geophys. Res. Earth Surf.* 120, 779–798.
- Wilcock, P.R., 1992. Flow competence: A criticism of a classic concept. *Earth Surf. Process. Landf.* 17, 289–298.
- Wilkinson, C., Harbor, D.J., Helgans, E., Kuehner, J.P., 2018. Plucking phenomena in nonuniform flow. *Geosphere* 14, 2157–2170.
- Williams, R., Reid, H., Brierley, G., 2019. Stuck at the bar: Larger-than-average grain lag deposits and the spectrum of particle mobility. *J. Geophys. Res. Earth Surf.* 124, 2751–2756.
- Wilson, A., Hovius, N., Turowski, J.M., 2013. Upstream-facing convex surfaces: Bedrock bedforms produced by fluvial bedload abrasion. *Geomorphology* 180, 187–204.
- Wilson, P., Matthews, J.A., Mourné, R.W., Linge, H., Olsen, J., 2020. Interpretation, age and significance of a relict paraglacial and periglacial boulder-dominated landform assemblage in Alnesdalen, Romsdalsalpane, southern Norway. *Geomorphology* 369, 107362.
- Wolman, M.G., 1954. A method of sampling coarse river-bed material. *EOS Trans. Am. Geophys. Union* 35, 951–956.
- Yager, E., Kirchner, J., Dietrich, W., 2007. Calculating bed load transport in steep boulder bed channels. *Water Resour. Res.* 43.
- Yager, E.M., Dietrich, W., Kirchner, J.W., McArdell, B., 2012. Prediction of sediment transport in step-pool channels. *Water Resour. Res.* 48.
- Yanites, B.J., Tucker, G.E., Mueller, K.J., Chen, Y.G., Wilcox, T., Huang, S.Y., Shi, K.W., 2010. Incision and channel morphology across active structures along the Peikang River, central Taiwan: Implications for the importance of channel width. *Geol. Soc. Am. Bull.* 122, 1192–1208.
- Yin, Y.H., Shyu, J.B.H., 2017. Sediment transport and erosional processes of a mountain bedrock channel using high-resolution topographic surveys. *EGUGA* 7791.
- Zimmermann, A., Church, M., Hassan, M.A., 2010. Step-pool stability: Testing the jammed state hypothesis. *J. Geophys. Res. Earth Surf.* 115.
- Zimmermann, A.E., Saletti, M., Zhang, C., Hassan, M.A., 2020. Step-pool channel features, in: *Reference Module in Earth Systems and Environmental Sciences*. Elsevier. URL: <http://www.sciencedirect.com/science/article/pii/B9780128182345000043>. <https://doi.org/10.1016/B978-0-12-818234-5.00004-3>.
- Zondervan, J.R., Stokes, M., Boulton, S.J., Telfer, M.W., Mather, A.E., 2020. Rock strength and structural controls on fluvial erodibility: Implications for drainage divide mobility in a collisional mountain belt. *Earth Planet. Sci. Lett.* 538, 116221.